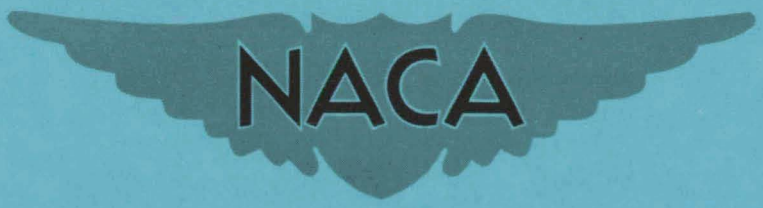

RESEARCH MEMORANDUM

EFFECTS OF TAPER RATIO ON THE LONGITUDINAL CHARACTERISTICS AT MACH NUMBERS FROM 0.6 TO 1.4 OF A WING-BODY-TAIL COMBINATION HAVING AN UNSWEPT WING OF ASPECT RATIO 3

By James L. Summers, Stuart L. Treon,
and Lawrence A. Graham

Ames Aeronautical Laboratory
Moffett Field, Calif.

NATIONAL ADVISORY COMMITTEE
FOR AERONAUTICS

WASHINGTON

March 23, 19.)
Declassified December 13, 1957

NATIONAL ADVISORY COMMITTEE FOR AERONAUTICS

RESEARCH MEMORANDUM

EFFECTS OF TAPER RATIO ON THE LONGITUDINAL CHARACTERISTICS AT MACH NUMBERS FROM 0.6 TO 1.4 OF A WING-BODY-TAIL COMBINATION HAVING AN UNSWEPT WING OF ASPECT RATIO 3

By James L. Summers, Stuart L. Treon, and Lawrence A. Graham

SUMMARY

The results of a wind-tunnel investigation to determine the effects of a variation in wing taper ratio on the longitudinal characteristics of a wing-body combination at Mach numbers from 0.6 to 1.4 and a Reynolds number of 1.5 million are presented. The wings were of aspect ratio 3 with an unswept midchord line and an NACA 64A003 profile. The wing-body combinations were tested both with and without a tail.

An increase in taper ratio from 0 to 1.0 had little effect on the variation with Mach number of the lift-curve slope, but had a marked effect on the variation with Mach number of the pitching-moment-curve slope. For a taper ratio of 0, the change in pitching-moment curve slope from 0.6 to 1.4 Mach number was indicative of a smooth rearward movement of the center of lift. For higher taper ratios, a forward shift of the center of lift occurred at subsonic Mach numbers to 0.92 followed by an abrupt rearward shift with further increase in Mach number; the over-all rearward movement from 0.6 to 1.4 Mach number was greater than that observed for the 0 taper ratio.

An increase in taper ratio from 0 to 0.5 resulted in an increased minimum drag coefficient and a decreased drag-rise factor at all Mach numbers, an increased maximum lift-drag ratio at subsonic Mach numbers and, generally, a reduced maximum lift-drag ratio at supersonic Mach numbers.

INTRODUCTION

The application of unswept wings to aircraft intended to operate at transonic and low supersonic Mach numbers has been rejected by some designers because these wings display large and abrupt movements of the center of lift at transonic Mach numbers. Calculations made employing the theory of reference 1 indicate a reduction of the center-of-lift travel with a reduction in taper ratio for wings with straight or sweptforward trailing edges. The present investigation was conducted in the Ames 2- by 2-foot transonic wind tunnel to determine the effects of a variation in wing taper ratio from 0 to 1.0 on the longitudinal characteristics of a wing-body combination employing a wing having an unswept 0.50-chord line and an aspect ratio of 3.

NOTATION

C_D	drag coefficient
$C_{D_{min}}$	minimum drag coefficient
C_L	lift coefficient
C_{L_α}	lift-curve slope
$C_{m_{c/4}}$	pitching-moment coefficient about quarter point of mean aerodynamic chord
c	local chord
$\bar{c}$	mean aerodynamic chord
$\left(\frac{L}{D}\right)_{max}$	maximum lift-drag ratio
l	length of body including portion removed to accommodate balance
M	free-stream Mach number
r	local radius of body
r_o	maximum radius of body
x	longitudinal distance from nose of body

$\frac{dC_m}{dC_L}$ pitching-moment-curve slope

ΔC_D drag coefficient less zero-lift drag coefficient

$\frac{\Delta C_D}{C_L^2}$ drag-rise factor

$\Delta\left(\frac{dC_m}{dC_L}\right)_M$ change in pitching-moment-curve slope due to change in Mach number, $\Delta\left(\frac{dC_m}{dC_L}\right)_M = \left(\frac{dC_m}{dC_L}\right) - \left(\frac{dC_m}{dC_L}\right)_{M=0.6}$

$\Delta\left(\frac{dC_m}{dC_L}\right)_{tail}$ change in pitching-moment-curve slope due to horizontal tail, $\Delta\left(\frac{dC_m}{dC_L}\right)_{tail} = \left(\frac{dC_m}{dC_L}\right)_{\substack{tail \\ on}} - \left(\frac{dC_m}{dC_L}\right)_{\substack{tail \\ off}}$, at an α for constant tail off C_L

α angle of attack, deg

λ taper ratio, $\frac{\text{tip chord}}{\text{root chord}}$

APPARATUS AND METHODS

The experimental study was made in the Ames 2- by 2-foot transonic wind tunnel which is fitted with a flexible nozzle followed by a ventilated test section (see fig. 1) which permits continuous choke-free operation from 0 to 1.4 Mach number.

Four wing-body models having wing taper ratios of 0, 0.25, 0.50, and 1.00 were constructed of steel. The wings were of aspect ratio 3 with NACA 64A003 airfoil sections normal to the unswept midchord line (fig. 2). The point of intersection of the wing midchord line with the body center line was common to all models. Each wing-body combination was tested with and without the tail assembly shown in figure 3. The models were mounted in the wind tunnel on a sting-supported internal strain-gage balance as shown in figure 4.

Lift and pitching moment for all taper ratios and drag for 0 and 0.5 taper ratio only were measured at angles of attack from -4° to approximately

13° and at Mach numbers from 0.6 to 1.4. A Reynolds number of 1.5 million, based on the mean aerodynamic chord of each model, was held constant for the tests. All coefficients were based on the wing area including the portion within the body. The pitching-moment coefficient was based on the mean aerodynamic chord and referred to the quarter-chord point. The measured drag was adjusted to correspond to a condition of free-stream static pressure acting at the model base.

Subsonic wall interference corrections, calculated on the basis of the theory of reference 2, were found to be small and therefore were not applied to the data. A discussion of the effect on the test results of reflected waves at low supersonic Mach numbers is contained in the Results and Discussion section. Corrections for air-stream angularity were not made since they were found to be less than the probable errors in measuring angle of attack. Drag corrections due to longitudinal pressure gradient were unnecessary throughout the test Mach number range since local Mach number deviations in the vicinity of the model were generally no greater than 0.003.

Apart from the small systematic errors due to neglecting the corrections discussed above, certain random errors of measurement exist which determine the precision or repeatability of the data. An analysis of the precision of the Mach number, angle of attack and lift, pitching-moment, and drag coefficients was made for the models of the present investigation, and the random uncertainties at three representative Mach numbers and two values of lift coefficient are presented in the following table:

	M = 0.8		M = 1.0		M = 1.2	
	$C_L = 0$	$C_L = 0.4$	$C_L = 0$	$C_L = 0.4$	$C_L = 0$	$C_L = 0.4$
M	±0.003	±0.003	±0.004	±0.004	±0.002	±0.002
α	±.02°	±.03°	±.02°	±.03°	±.02°	±.03°
C_L	±.005	±.010	±.005	±.006	±.003	±.006
$C_{m_{c/4}}$	±.004	±.006	±.004	±.005	±.003	±.005
C_D	±.0003	±.0010	±.0003	±.0006	±.0003	±.0006

RESULTS AND DISCUSSION

Variations of lift coefficient with angle of attack, pitching-moment coefficient, and drag coefficient at Mach numbers from 0.6 to 1.4 are presented in figures 5, 6, and 7, respectively, for the wing-body combinations, and in figures 8, 9, and 10, for the wing-body-tail combinations. The asymmetry of the curves about zero lift in some of the figures is attributed to small inaccuracies of model construction.

Lift and Pitching-Moment Characteristics

The variations with Mach number of lift-curve slope and pitching-moment-curve slope for three values of lift coefficient are shown for the tail-off configurations in figure 11 and for the tail-on configurations in figure 12. The irregularities in the curves which appear at low supersonic Mach numbers are considered to be the result of reflections from the tunnel walls of the shock waves emanating from the body nose and wing leading edge which impinge upon the rear portion of the models. These irregularities are slightly larger in magnitude in the data for the tail-on configurations because of the influence of the reflected waves on the horizontal surface.

In order to assess the magnitude of the effects of shock-wave reflections on model characteristics, an investigation was conducted on three models differing only in size. The projected frontal areas of the models were 0.09, 0.51, and 1.15 percent of the test section cross-sectional area. The results of this study indicated that for models of the size employed in the present investigation (about 0.51-percent blockage), the influence of the reflected waves on the model characteristics was small and confined to the Mach number range from 1.00 to 1.15. The magnitude of the effects of the reflected waves is considered not sufficiently great to affect the conclusions drawn from the results.

The calculated values of lift-curve and pitching-moment-curve slopes for the configurations without the tail, shown in figure 11, were based on the theory of reference 1. This theory takes into account wing-body interference and employs values of wing alone lift-curve slope at subsonic, sonic, and supersonic Mach numbers as obtained from references 3, 4, and 5, respectively. Qualitative agreement is noted between the calculated and experimental values of lift-curve slope and pitching-moment-curve slope for the Mach number range of the present investigation. The greatest discrepancy between theory and experiment is seen to be in the Mach numbers for which the maximum value of lift-curve slope and the most positive value of pitching-moment curve slope occurs. The calculated values occur at Mach numbers approximately 0.1 higher than the experimental values. This discrepancy is probably a result of the inability of the theory to account for the fact that local sonic and supersonic flow was established prior to the establishment of these conditions in the free stream.

An examination of figures 11 and 12 indicates that an increase in taper ratio had no unusual effect on the variation of lift-curve slope with Mach number, but had a marked effect on the variation of pitching-moment-curve slope with Mach number at lift coefficients from 0 to 0.4. These effects are shown more clearly in figures 13 and 14 where the lift-curve slopes and incremental pitching-moment-curve slopes for the four values of taper ratio are compared for the tail-off and tail-on

configurations, respectively. Generally, lower lift-curve slopes are displayed by the 0 taper ratio configuration, particularly for 0.4 lift coefficient at subsonic Mach numbers. For taper ratios greater than 0, there is little difference in the values of lift-curve slope.

The change in pitching-moment-curve slope due to change in Mach number, $\Delta\left(\frac{dC_m}{dC_L}\right)_M$, was chosen as the parameter in figures 13(b) and 14(b) to indicate the effects of taper ratio on the pitching-moment characteristics. For a taper ratio of 0, the change in pitching-moment-curve slope with Mach number indicates a relatively smooth rearward movement of the center of lift with increasing Mach number, the over-all movement from 0.6 to 1.4 Mach number being about 16 percent of the mean aerodynamic chord at 0 lift coefficient (fig. 13(b)). For taper ratios from 0.25 to 1.00 at 0 lift, an increase in Mach number from 0.60 to 0.92 resulted in a forward movement of the center of lift of about 8 percent of the mean aerodynamic chord followed by a rearward movement of approximately 27 percent of the mean aerodynamic chord as the Mach number was increased to 1.4. This movement was abrupt at Mach numbers between 0.9 and 1.0. At lift coefficients greater than 0, the variation with Mach number of the increment of pitching-moment-curve slope is generally similar to that for 0 lift coefficient although at 0.2 lift coefficient, essentially the same variation from 0.6 to 1.4 Mach number is noted for all values of taper ratio. A comparison of figures 13(b) and 14(b) indicates that although the over-all change in pitching-moment-curve slope is greater for the tail-on configurations, the variation with Mach number is essentially the same with or without the horizontal tail. The contribution of the unswept horizontal tail to the static longitudinal stability is shown in figure 15 where the increment of pitching-moment-curve slope due to the tail is plotted as a function of Mach number. The least over-all increase in stability due to the tail from 0.6 to 1.4 Mach number is noted for the taper ratio of 0. Also apparent is the destabilizing effect of the unswept horizontal tail (for all values of wing taper ratio) at Mach numbers from approximately 0.90 to 1.05.

Drag Characteristics

The variations with Mach number of minimum drag coefficient, drag-rise factor, and maximum lift-drag ratio for taper ratios of 0 and 0.5 are shown in figure 16 for the tail-off configurations and in figure 17 for the tail-on configurations. Drag-rise factor was determined from the slope of curves of drag coefficient plotted against lift coefficient squared over the linear range from 0 to 0.4 lift coefficient. An increase in taper ratio from 0 to 0.5 resulted in an increase in the minimum drag coefficient and a decrease in the drag-rise factor (particularly at subsonic Mach numbers) throughout the test Mach number range. In general,

higher maximum lift-drag ratios are observed at subsonic Mach numbers for the 0.5 taper ratio and at supersonic Mach numbers for the 0 taper ratio.

CONCLUSIONS

The results of an experimental investigation made to assess the effects of a variation in wing taper ratio on the lift, pitching-moment, and drag characteristics of an unswept, aspect ratio 3, wing-body combination at Mach numbers from 0.6 to 1.4 indicate:

1. An increase in wing taper ratio from 0 to 1.0 had no unusual effect on the variation of lift-curve slope with Mach number although lower values of lift-curve slope were observed for a taper ratio of 0, particularly for 0.4 lift coefficient at subsonic Mach numbers.

2. For a taper ratio of 0, an increase in Mach number from 0.6 to 1.4 resulted in a gradual rearward shift of the center of lift of about 16 percent of the mean aerodynamic chord at 0 lift coefficient. For taper ratios from 0.25 to 1.00 at 0 lift, an increase in Mach number from 0.60 to 0.92 resulted in a forward movement of the center of lift of about 8 percent of the mean aerodynamic chord followed by a rearward movement of approximately 27 percent of the mean aerodynamic chord as the Mach number was increased to 1.4. This movement was abrupt at Mach numbers between 0.9 and 1.0.

3. The change in longitudinal stability from 0.6 to 1.4 Mach number due to an unswept horizontal tail was least for a wing taper ratio of 0.

4. The horizontal tail was destabilizing for all values of taper ratio at Mach numbers from approximately 0.90 to 1.05.

5. An increase in taper ratio from 0 to 0.5 resulted in an increase in the minimum drag coefficient and a decrease in the drag-rise factor throughout the test Mach number range.

6. An increase in taper ratio from 0 to 0.5 resulted in an increase in the maximum lift-drag ratio at subsonic Mach numbers and, generally, a decrease at supersonic Mach numbers.

Ames Aeronautical Laboratory
National Advisory Committee for Aeronautics
Moffett Field, Calif., Dec. 20, 1954

REFERENCES

1. Nielsen, Jack N., Kaattari, George E., and Anastasio, Robert F.: A Method for Calculating the Lift and Center of Pressure of Wing-Body-Tail Combinations at Subsonic, Transonic, and Supersonic Speeds. NACA RM A53G08, 1953.

2. Baldwin, Barrett S., Jr., Turner, John B., and Knechtel, Earl D.: Wall Interference in Wind Tunnels With Slotted and Porous Boundaries at Subsonic Speeds. NACA TN 3176, 1954.

3. DeYoung, John, and Harper, Charles W.: Theoretical Symmetric Span Loading at Subsonic Speeds for Wings Having Arbitrary Plan Form. NACA Rep. 921, 1948.

4. Jones, Robert T.: Properties of Low-Aspect-Ratio Pointed Wings at Speeds Below and Above the Speed of Sound. NACA Rep. 835, 1946.

5. Lapin, Ellis: Charts for the Computation of Lift and Drag of Finite Wings at Supersonic Speeds. Douglas Aircraft Company, Rep. No. SM-13480, 1949.

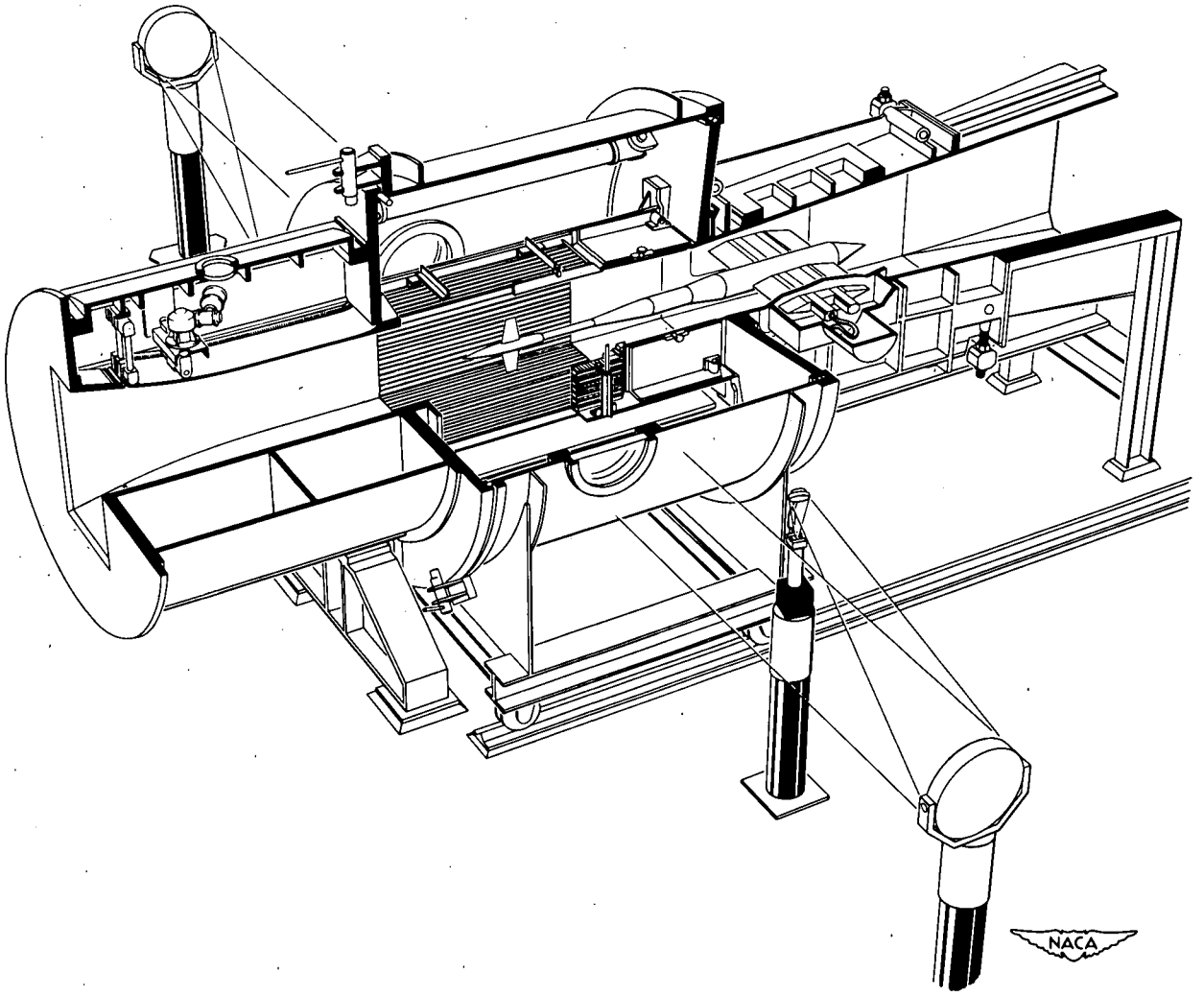

Figure 1.- Test section of the Ames 2-by 2-foot transonic wind tunnel.

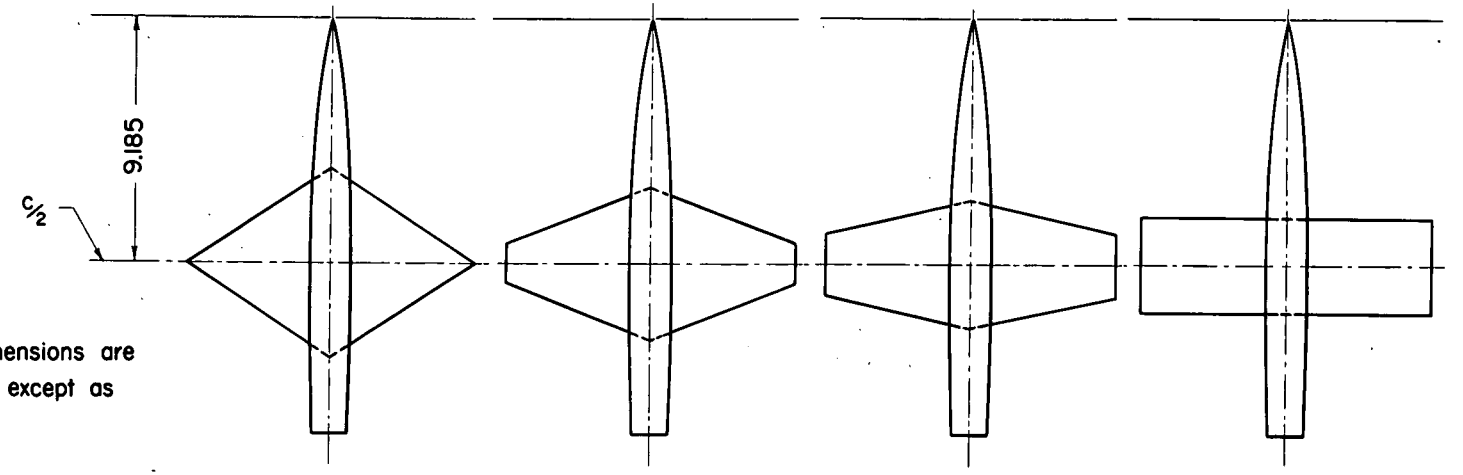

Note: All dimensions are in inches except as noted.

Taper ratio	0	0.25	0.50	1.00
Airfoil section (streamwise)	NACA 64A003	NACA 64A003	NACA 64A003	NACA 64A003
Aspect ratio	3.00	3.00	3.00	3.00
Span	10.794	10.794	10.794	10.794
Tip chord	0	1.438	2.398	3.597
Root chord (at body ℄)	7.165	5.750	4.796	3.597
Mean aerodynamic chord	4.780	4.028	3.751	3.597
Wing area	38.81	38.81	38.81	38.81

Figure 2.- Plan views and geometric details of the wing-body models.

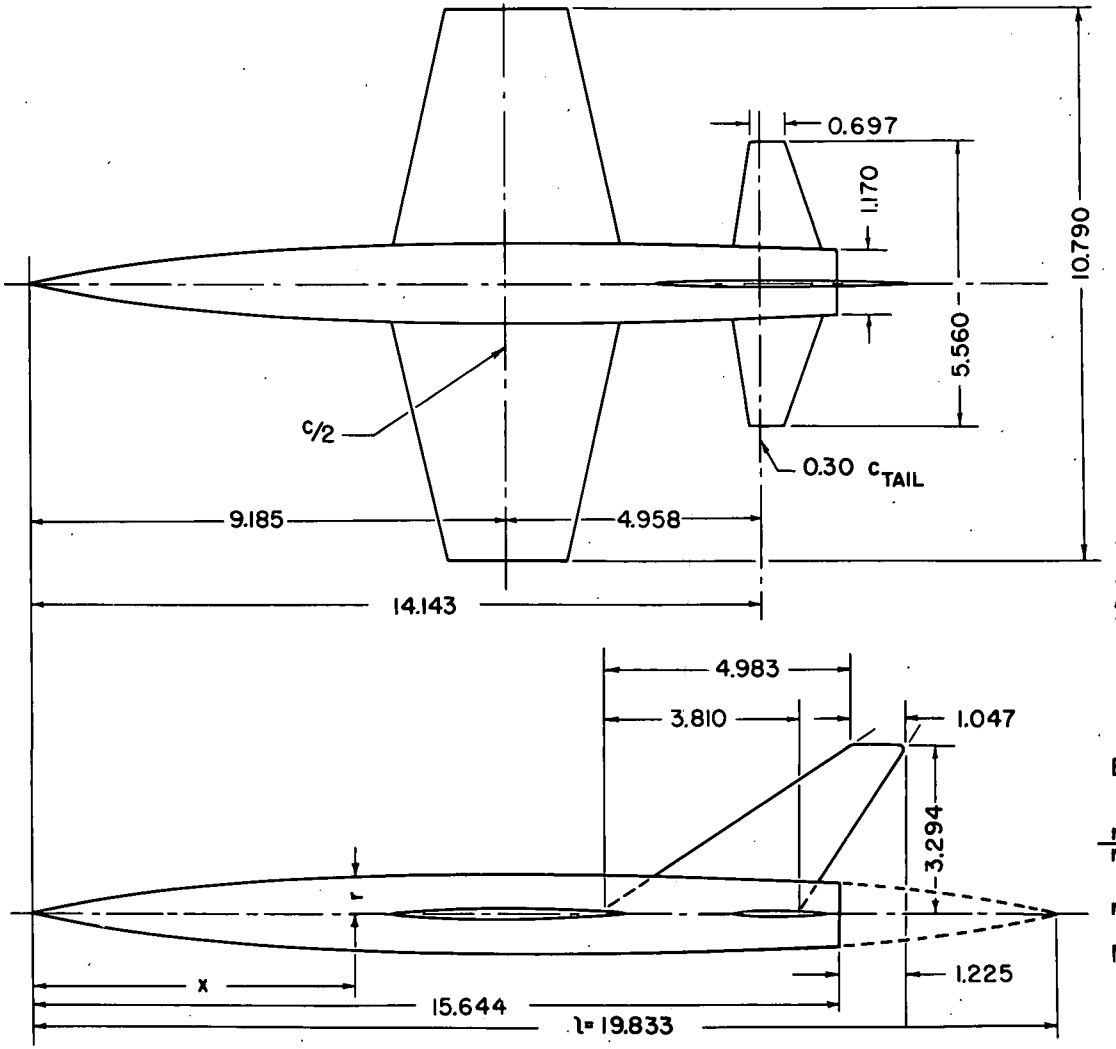

Horizontal Tail:

Taper ratio	0.33
Aspect ratio	4.00
Area	7.76
Thickness ratio	0.03

Body:

$$\frac{r}{r_o} = \left[1 - \left(1 - \frac{2x}{l}\right)^2\right]^{3/4}$$

$r_o = 0.794$

Note: All dimensions are in inches except as noted.

Figure 3.- Details of a plan view and a side view of a typical wing-body-tail model.

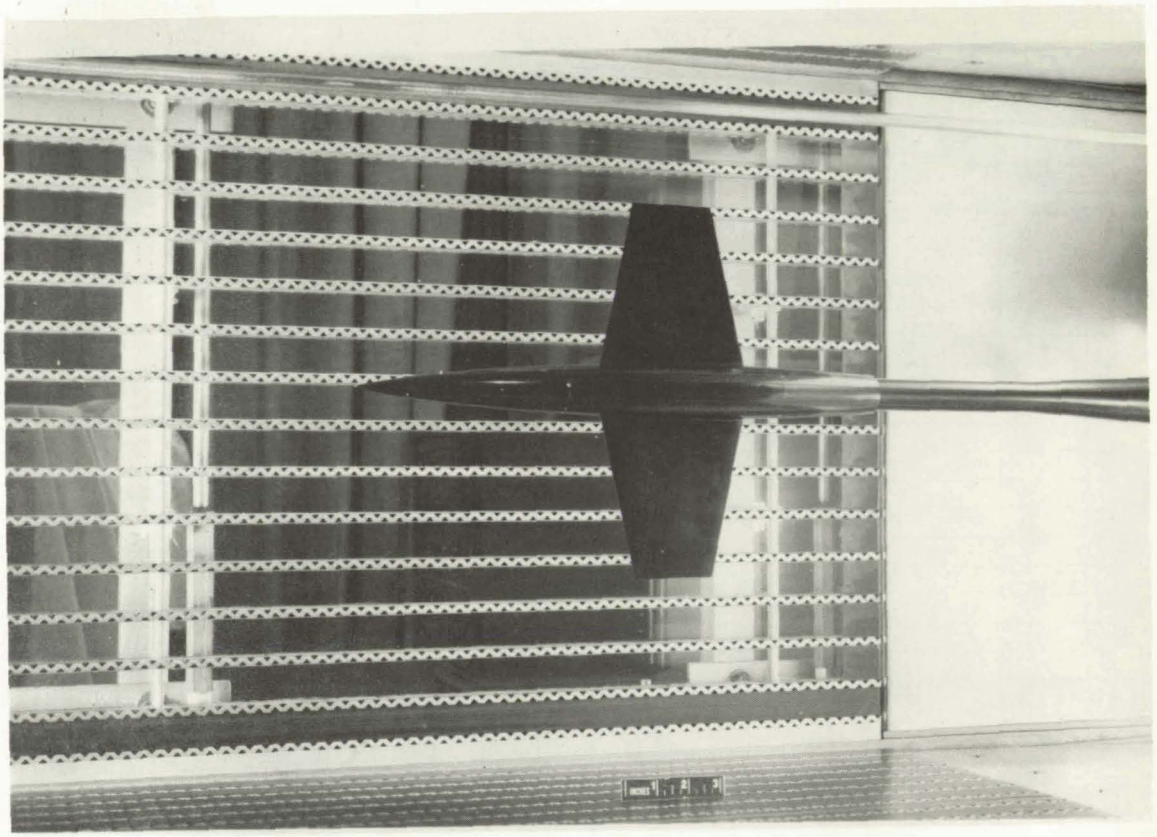

A-19209

Figure 4.- Typical model installation in the Ames 2- by 2- foot transonic wind tunnel.

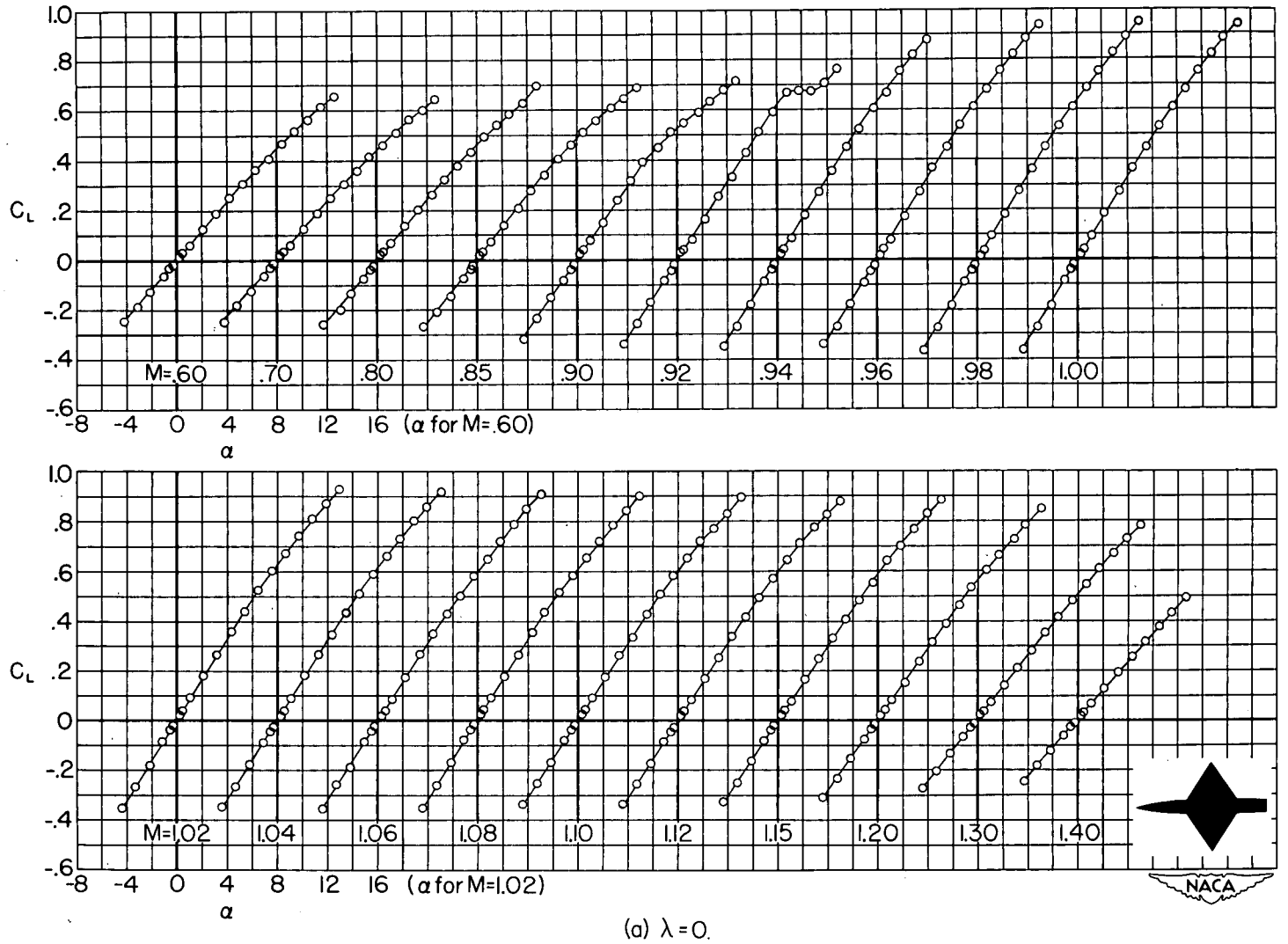

(a) $\lambda = 0$.

Figure 5.- Variation of lift coefficient with angle of attack at constant Mach number for an unswept wing-body combination.

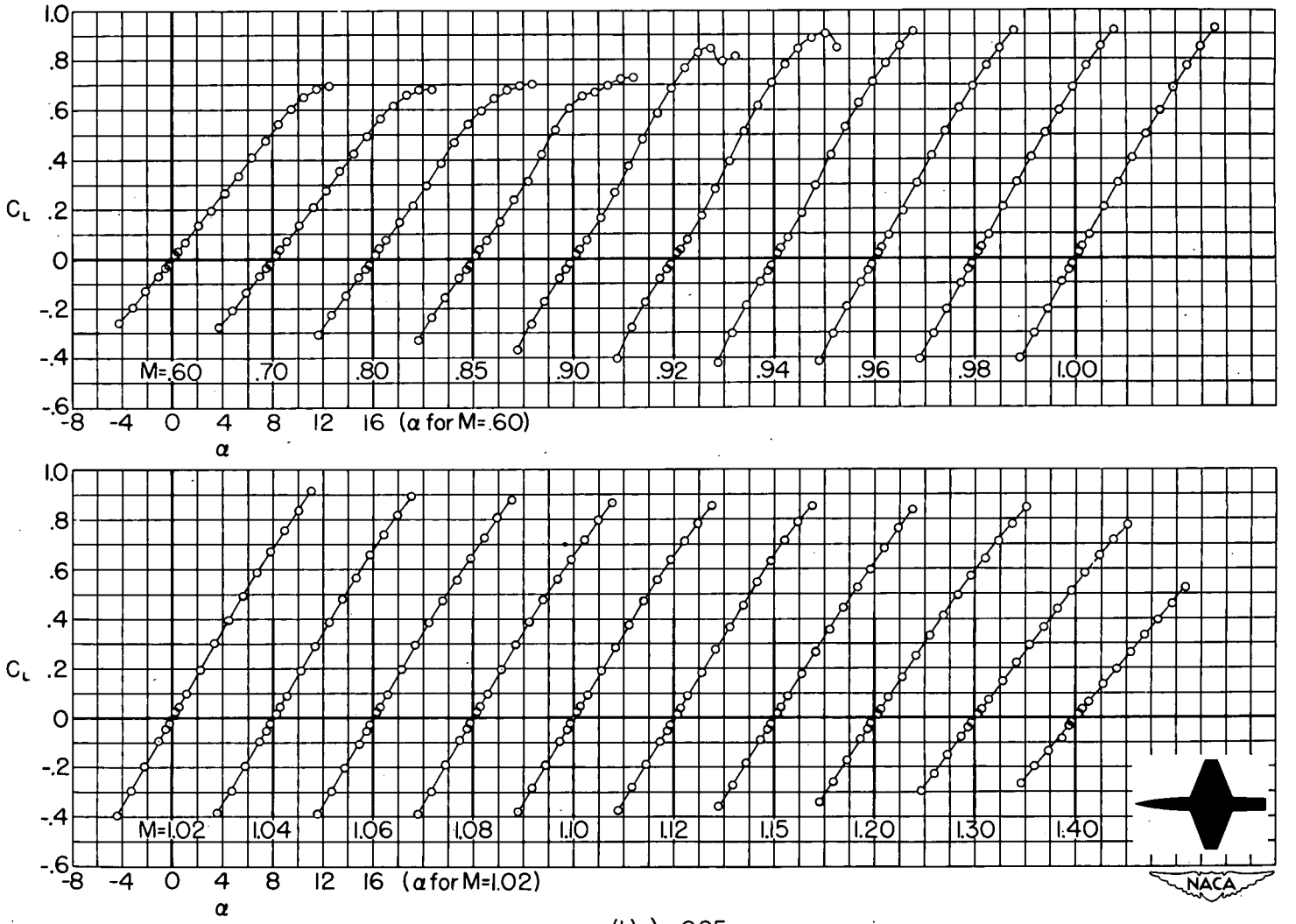

(b) $\lambda = 0.25$.

Figure 5.- Continued.

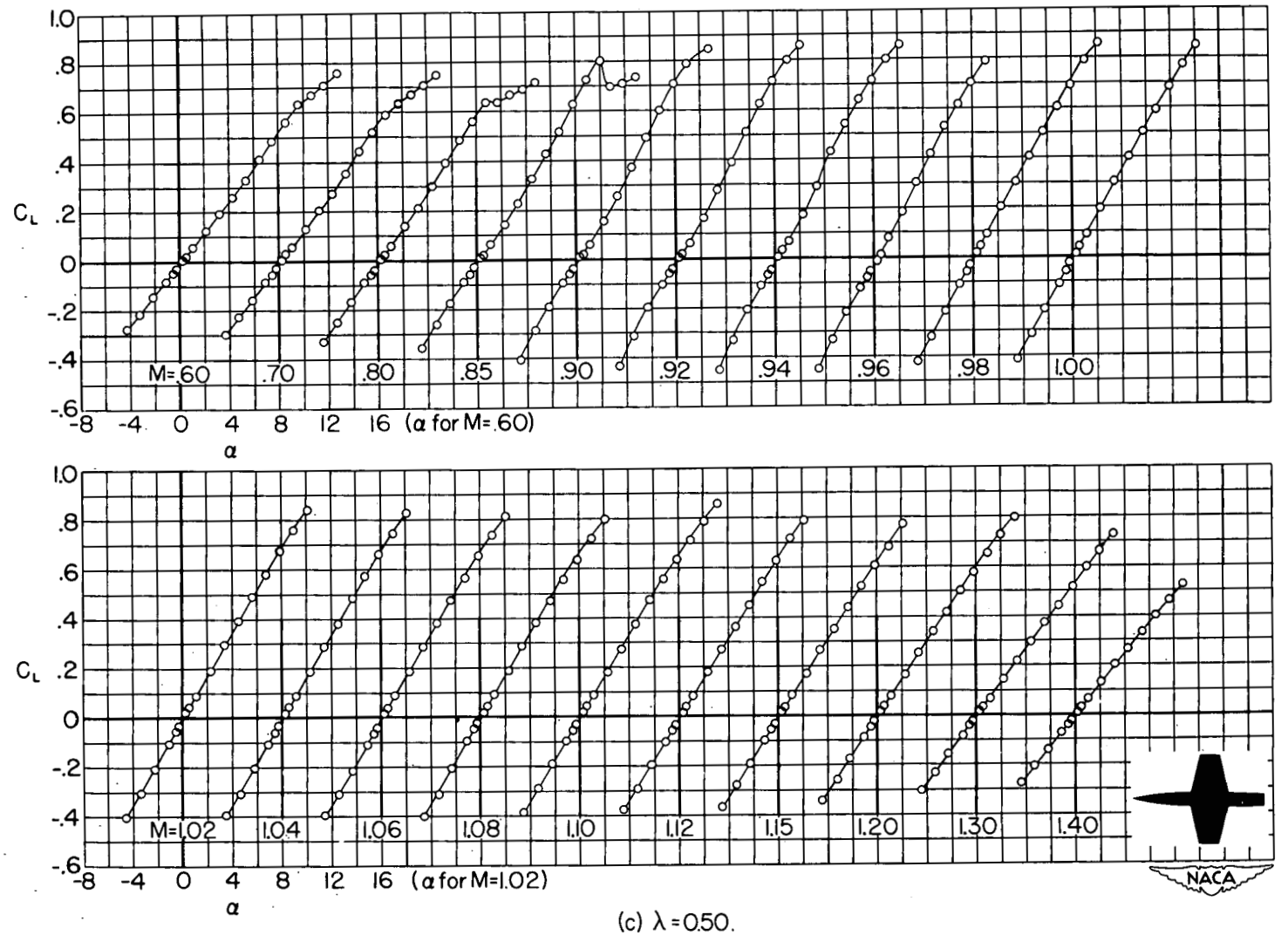

(c) $\lambda = 0.50$.

Figure 5.- Continued.

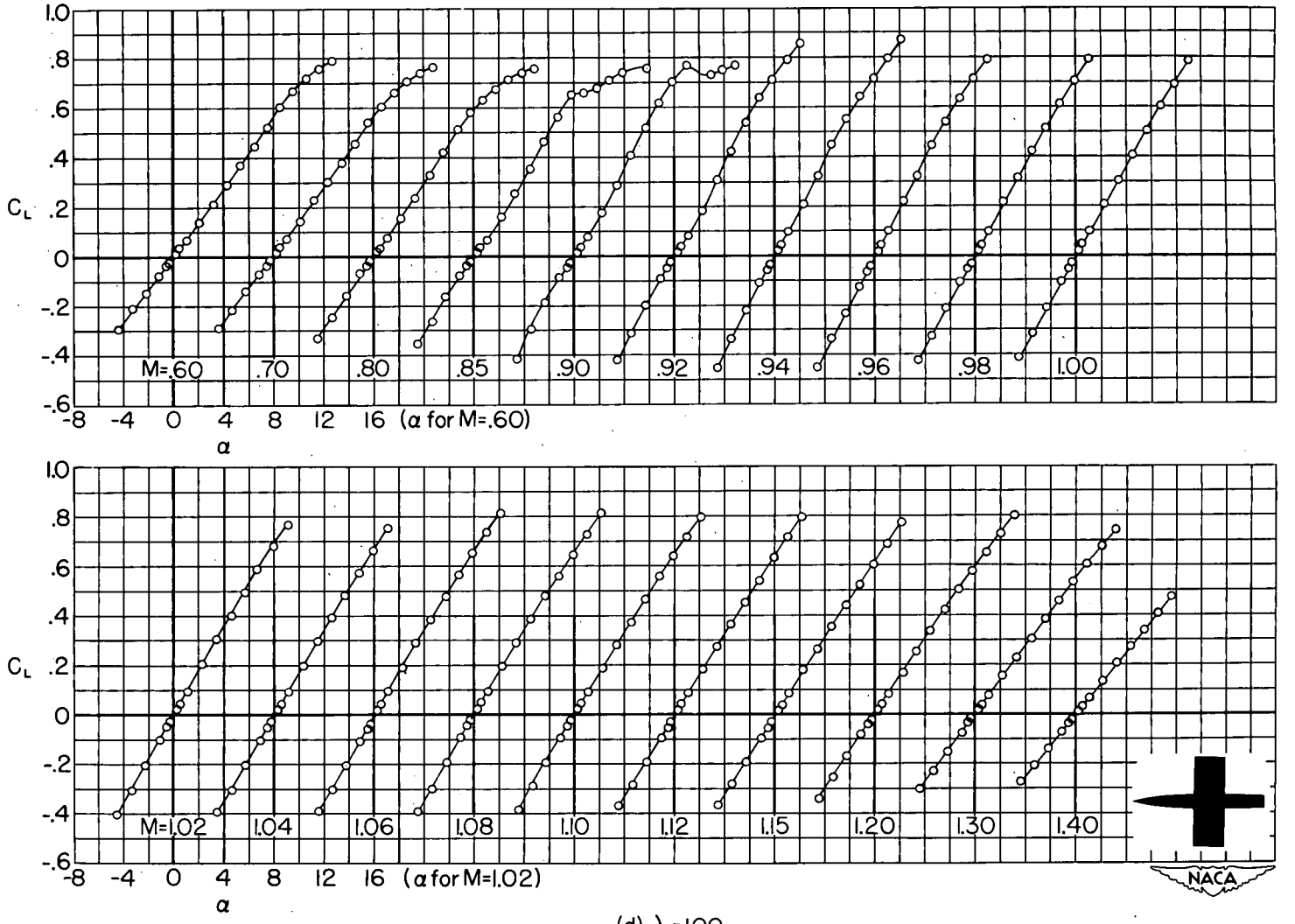

(d) $\lambda = 1.00$.

Figure 5.- Concluded.

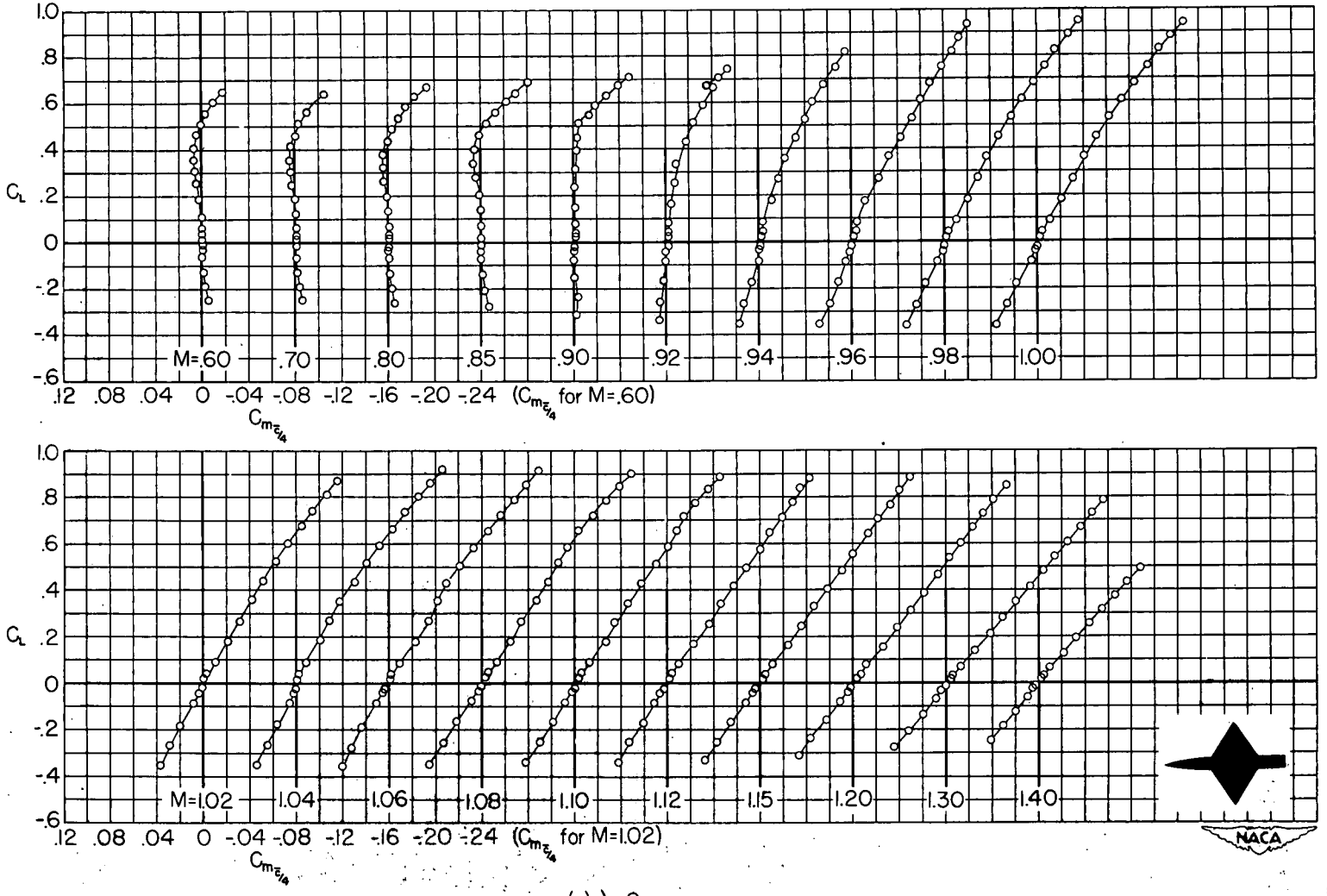

(a) $\lambda = 0$.

Figure 6.- Variation of lift coefficient with pitching-moment coefficient at constant Mach number for an unswept wing-body combination.

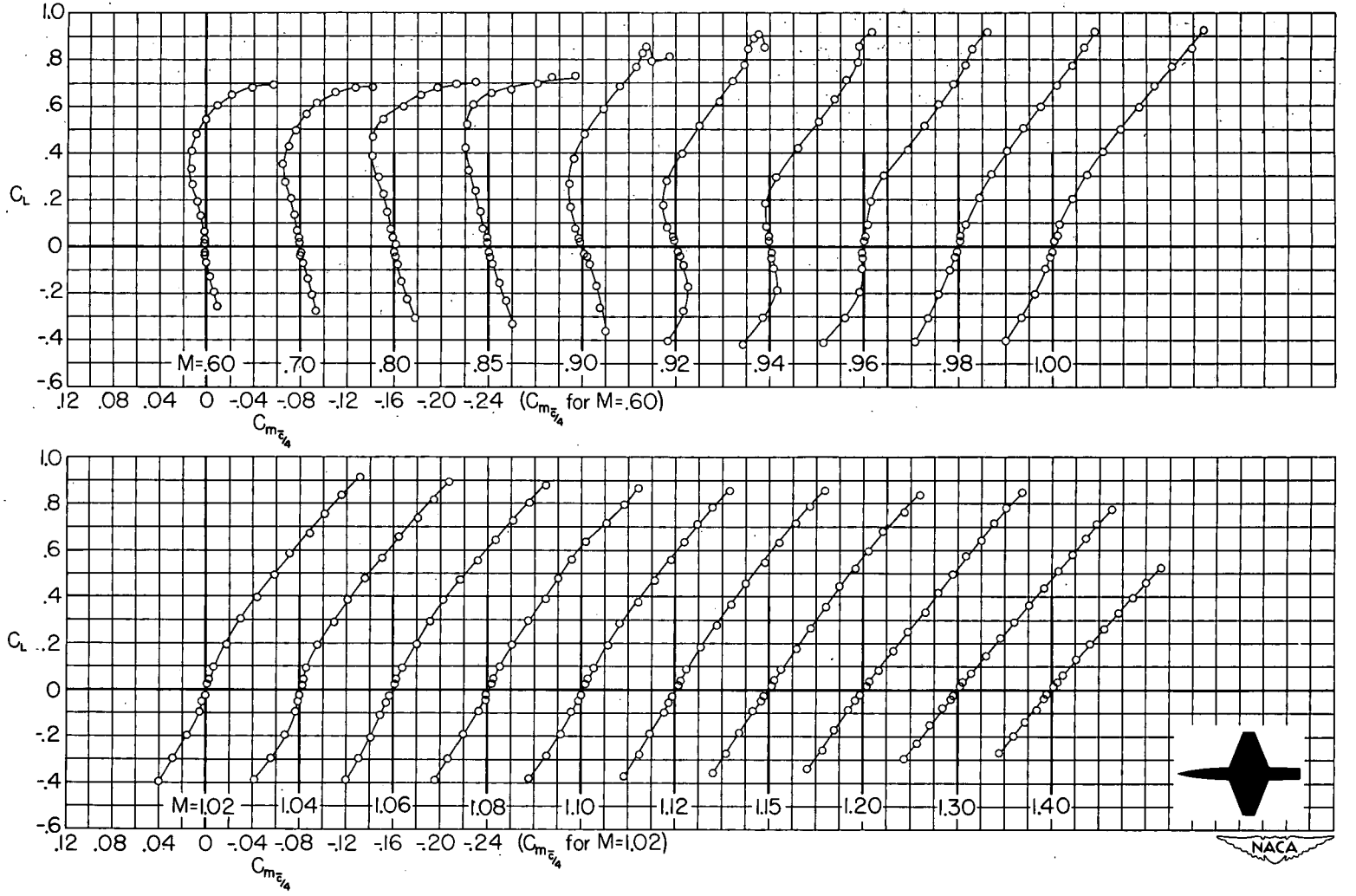

(b) $\lambda = 0.25$.

Figure 6.- Continued.

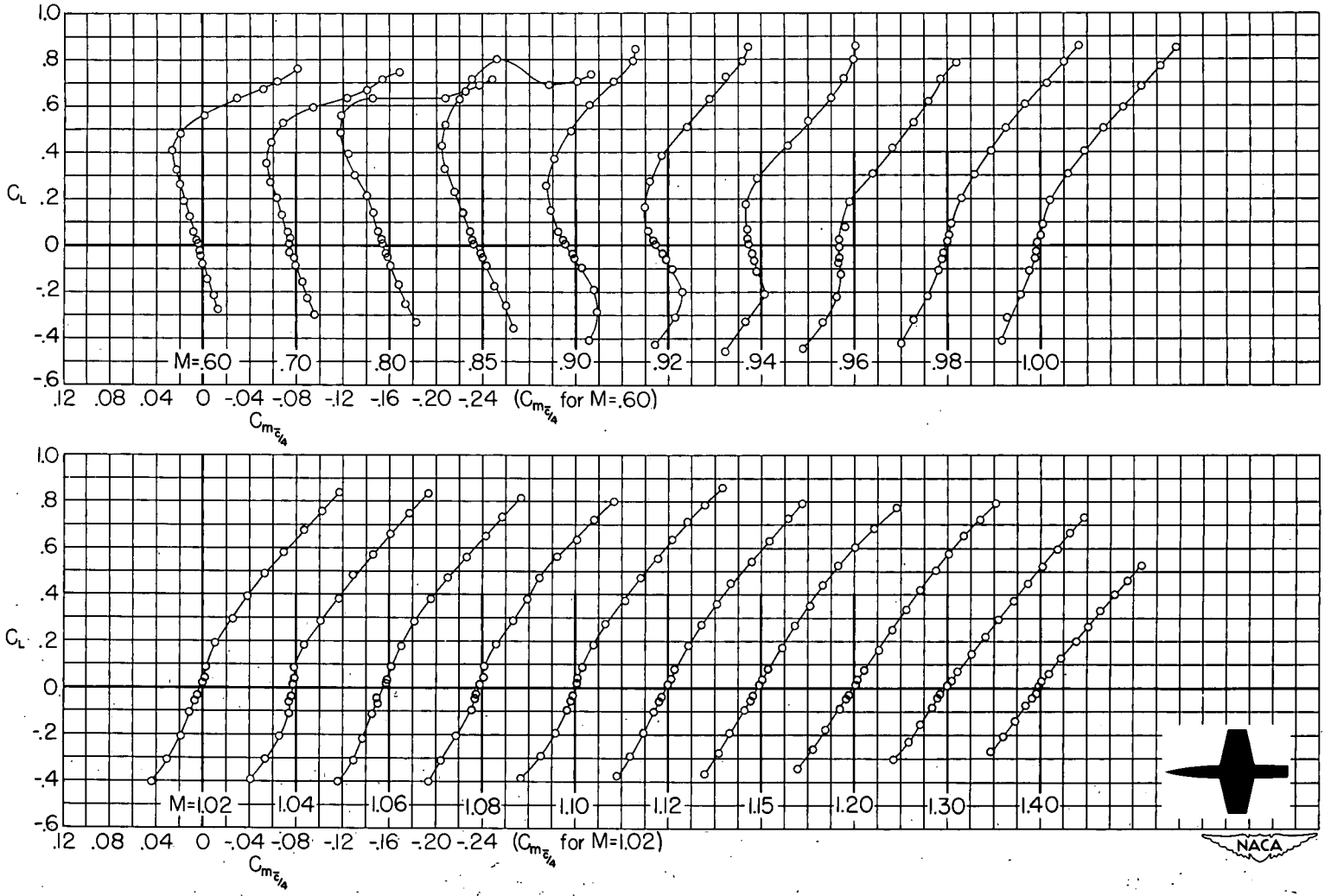

(c) $\lambda = 0.50$.

Figure 6.- Continued.

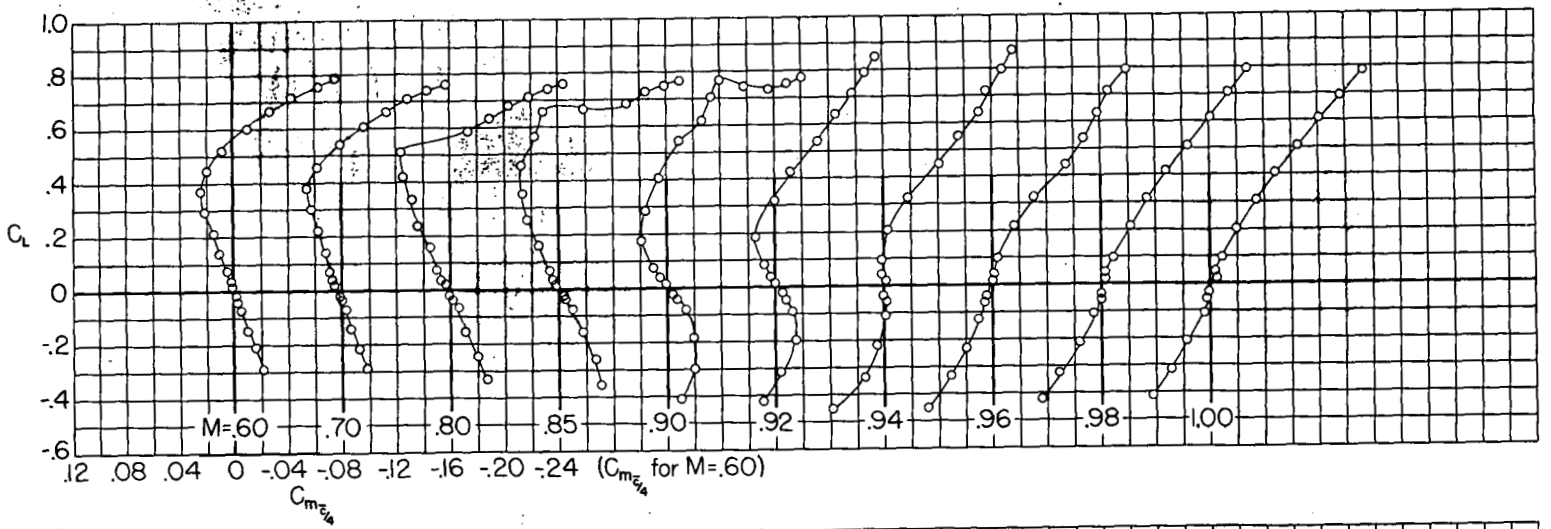

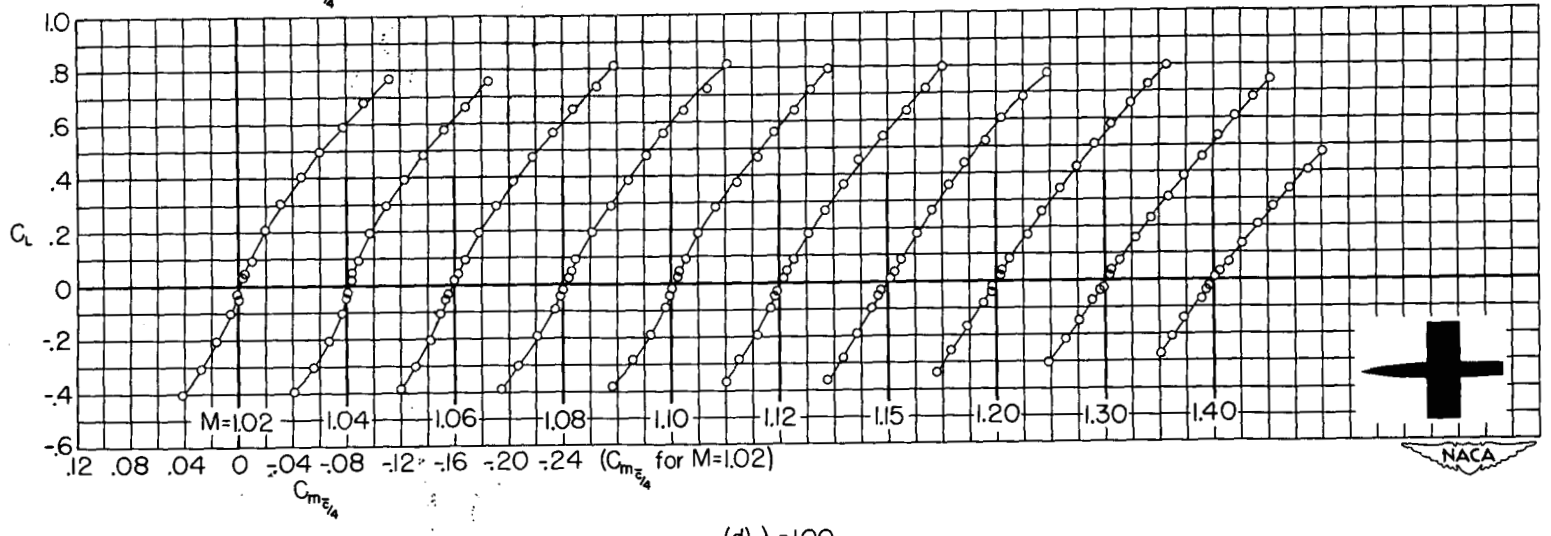

(d) $\lambda = 1.00$

Figure 6.- Concluded.

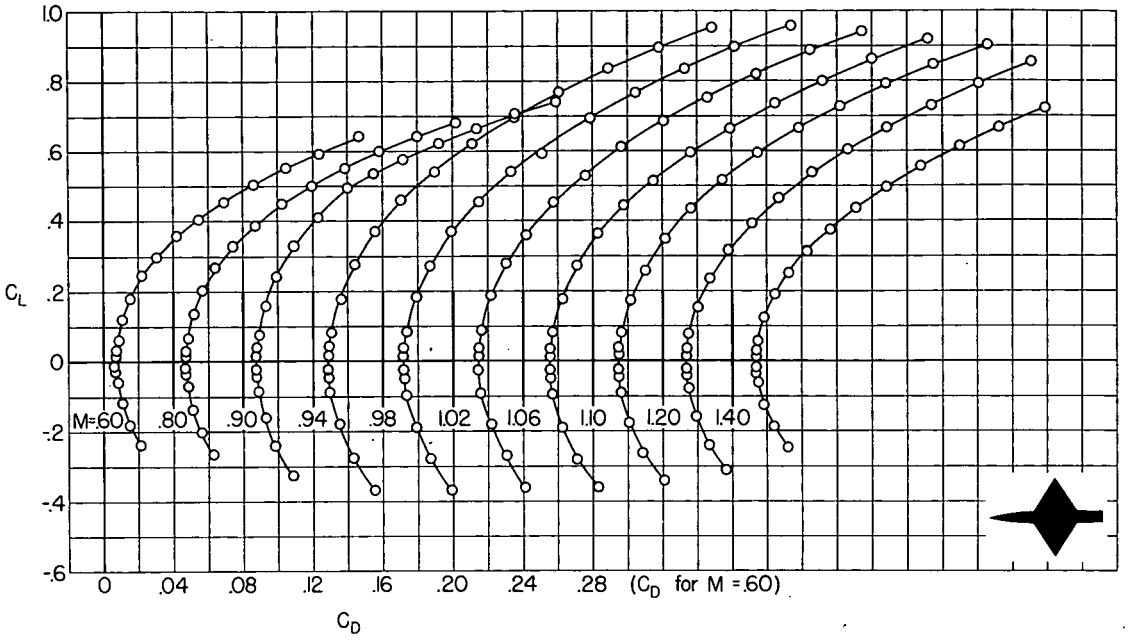

(a) $\lambda = 0.$

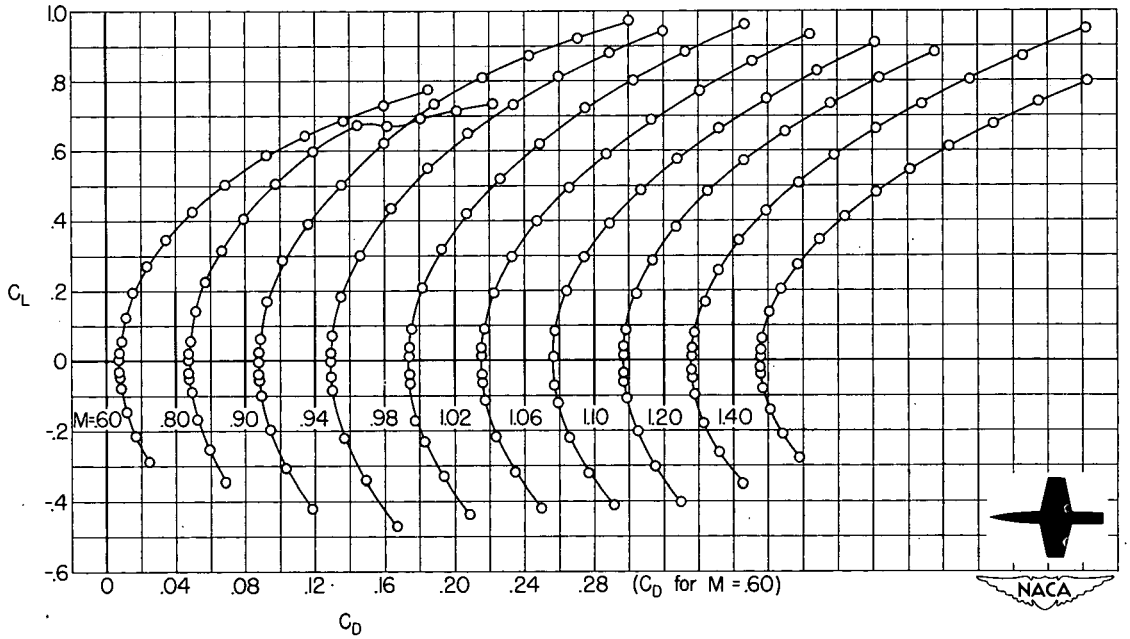

(b) $\lambda = 0.50.$

Figure 7.- Variation of lift coefficient with drag coefficient at constant Mach number for an unswept wing-body combination.

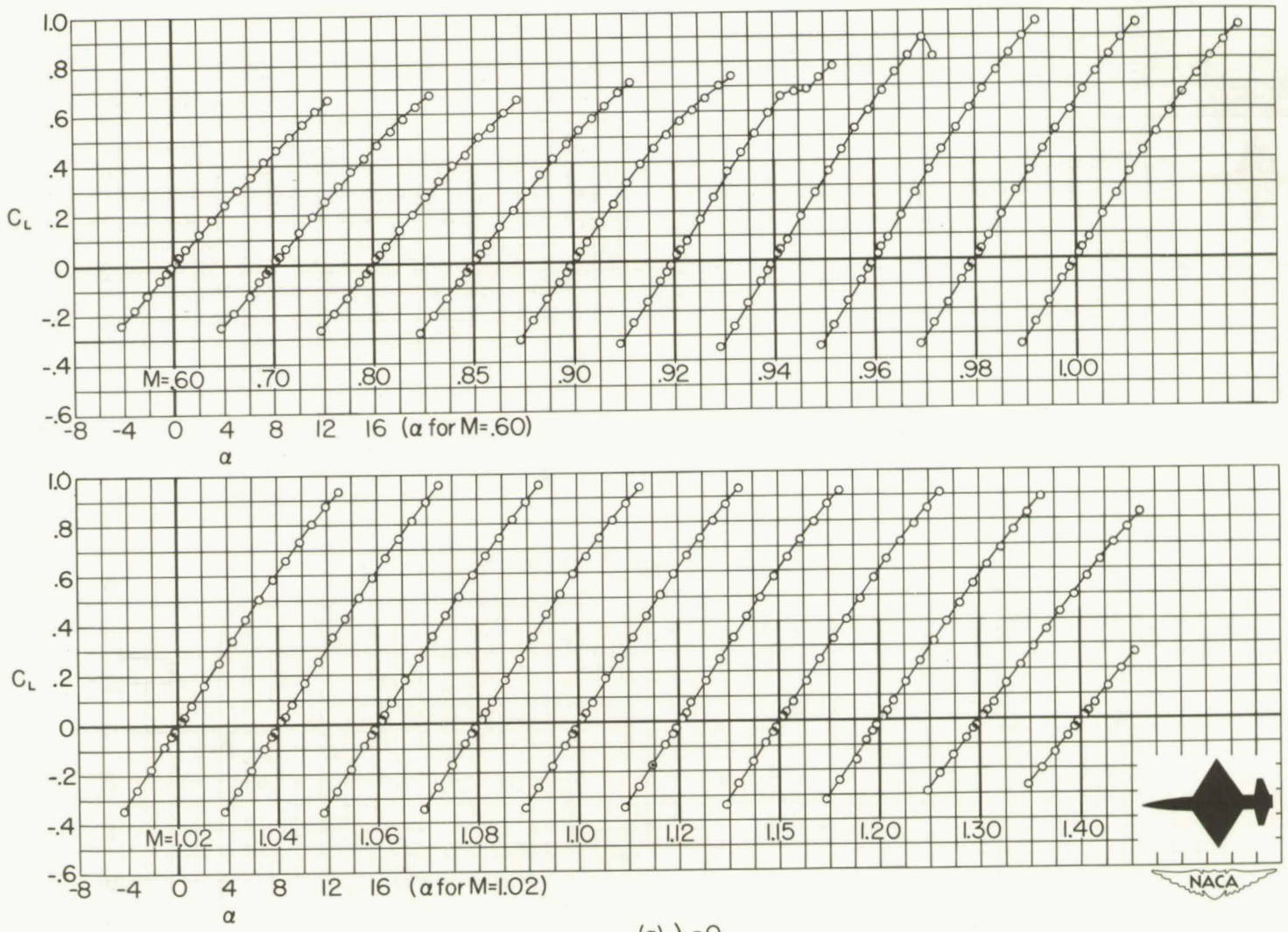

(a) $\lambda = 0$.

Figure 8.- Variation of lift coefficient with angle of attack at constant Mach number for an unswept wing-body-tail combination.

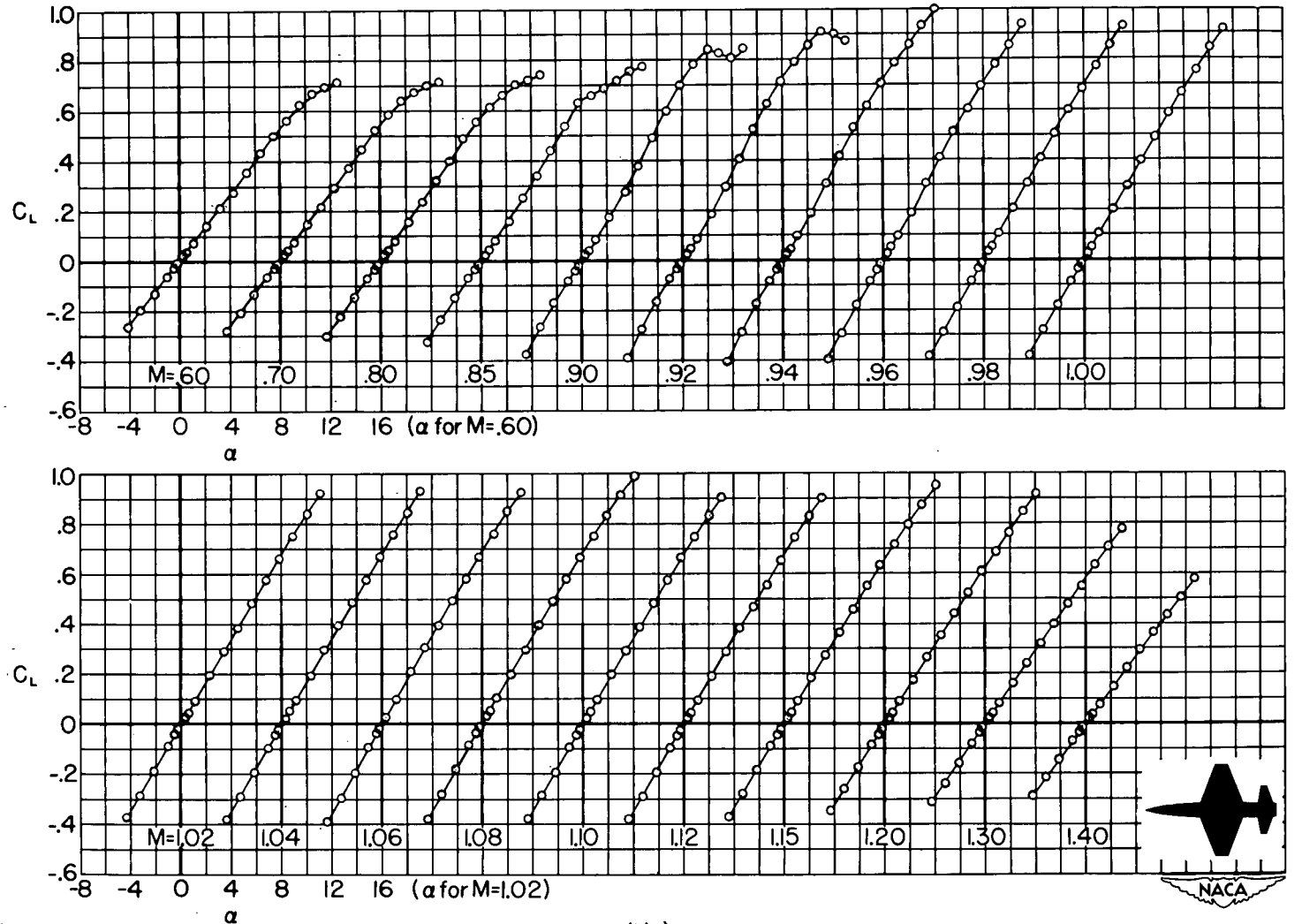

(b) $\lambda = 0.25$.

Figure 8.- Continued.

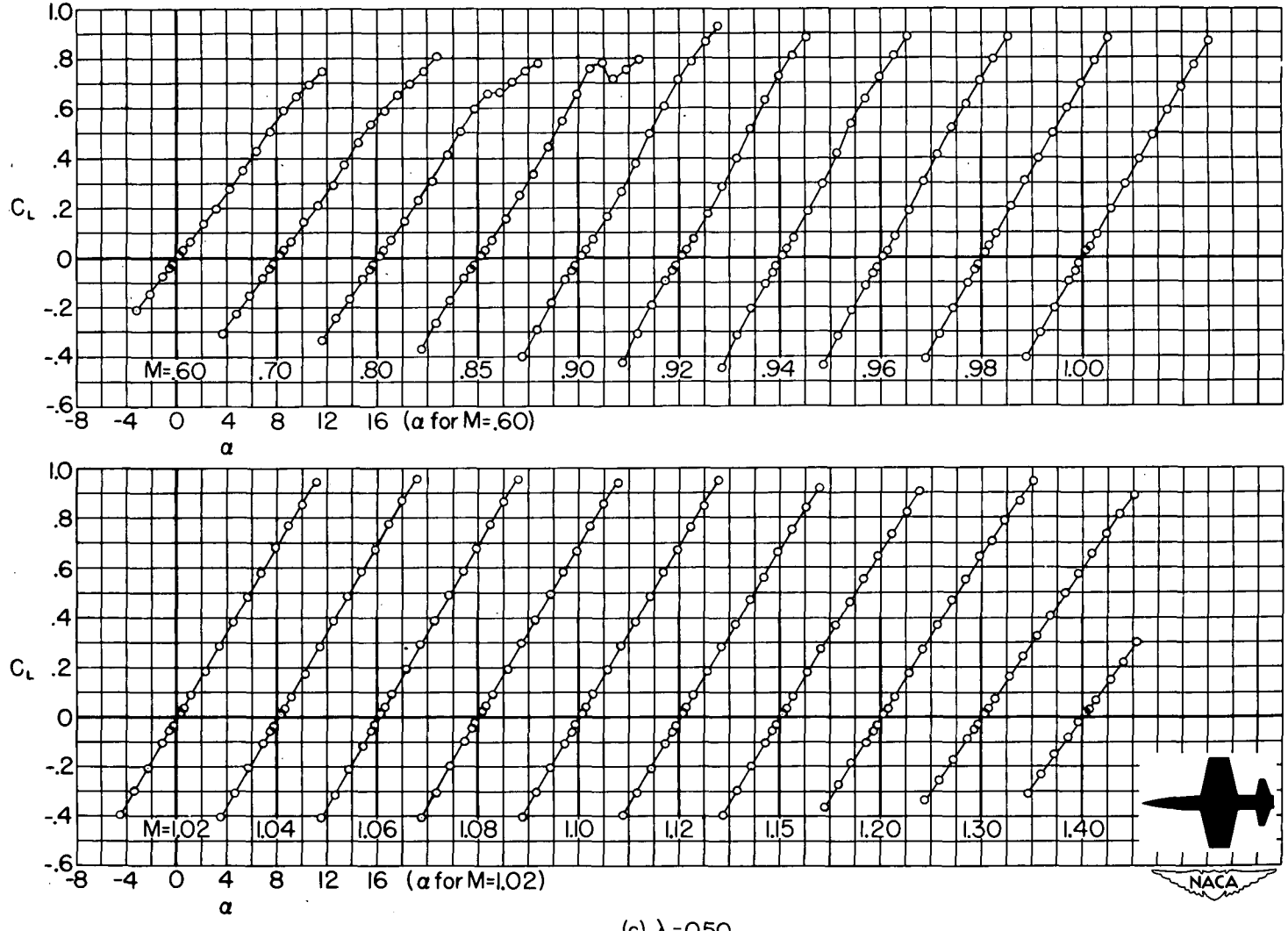

(c) $\lambda = 0.50$.

Figure 8.- Continued.

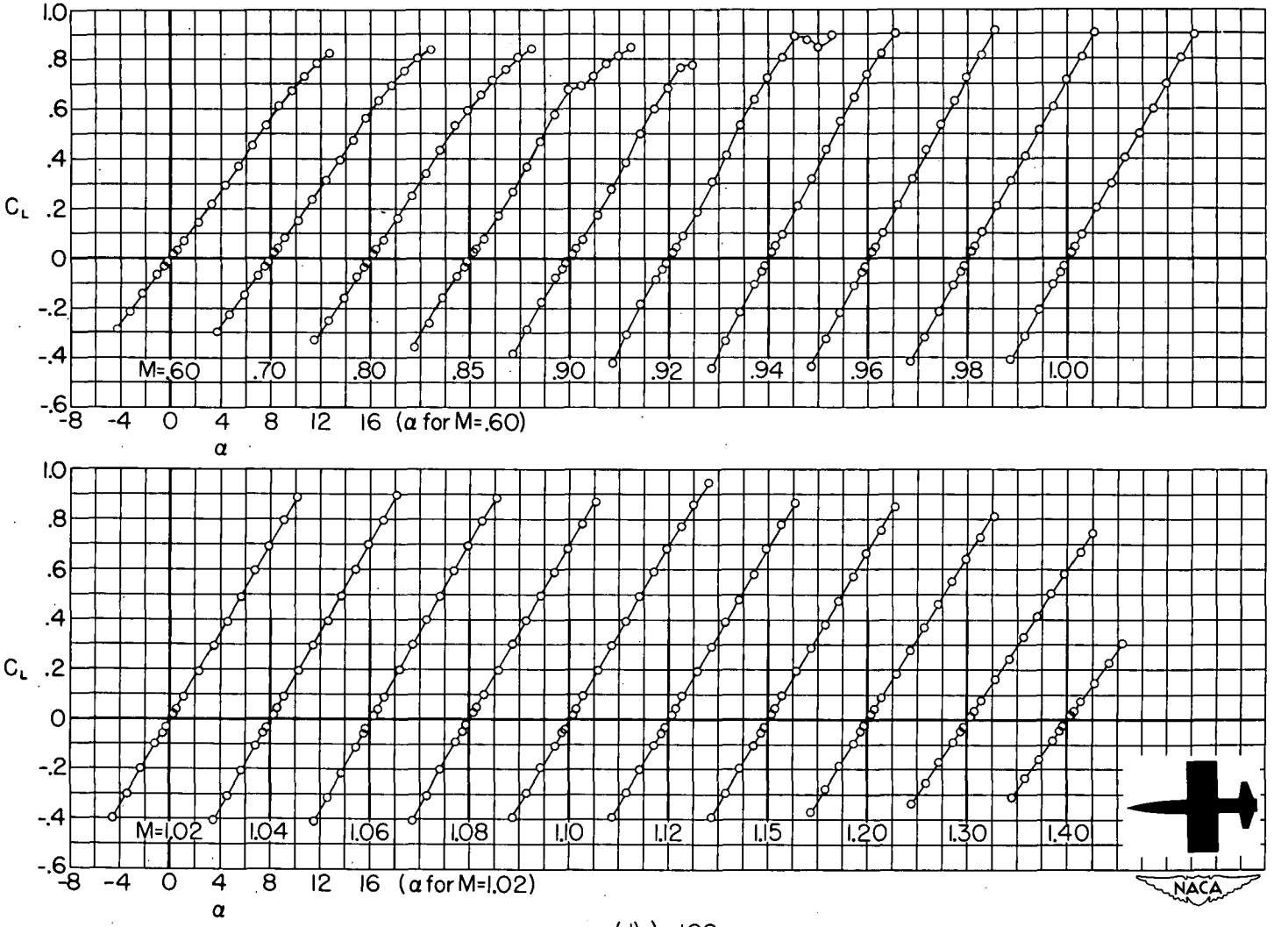

(d) $\lambda = 1.00$.

Figure 8.- Concluded.

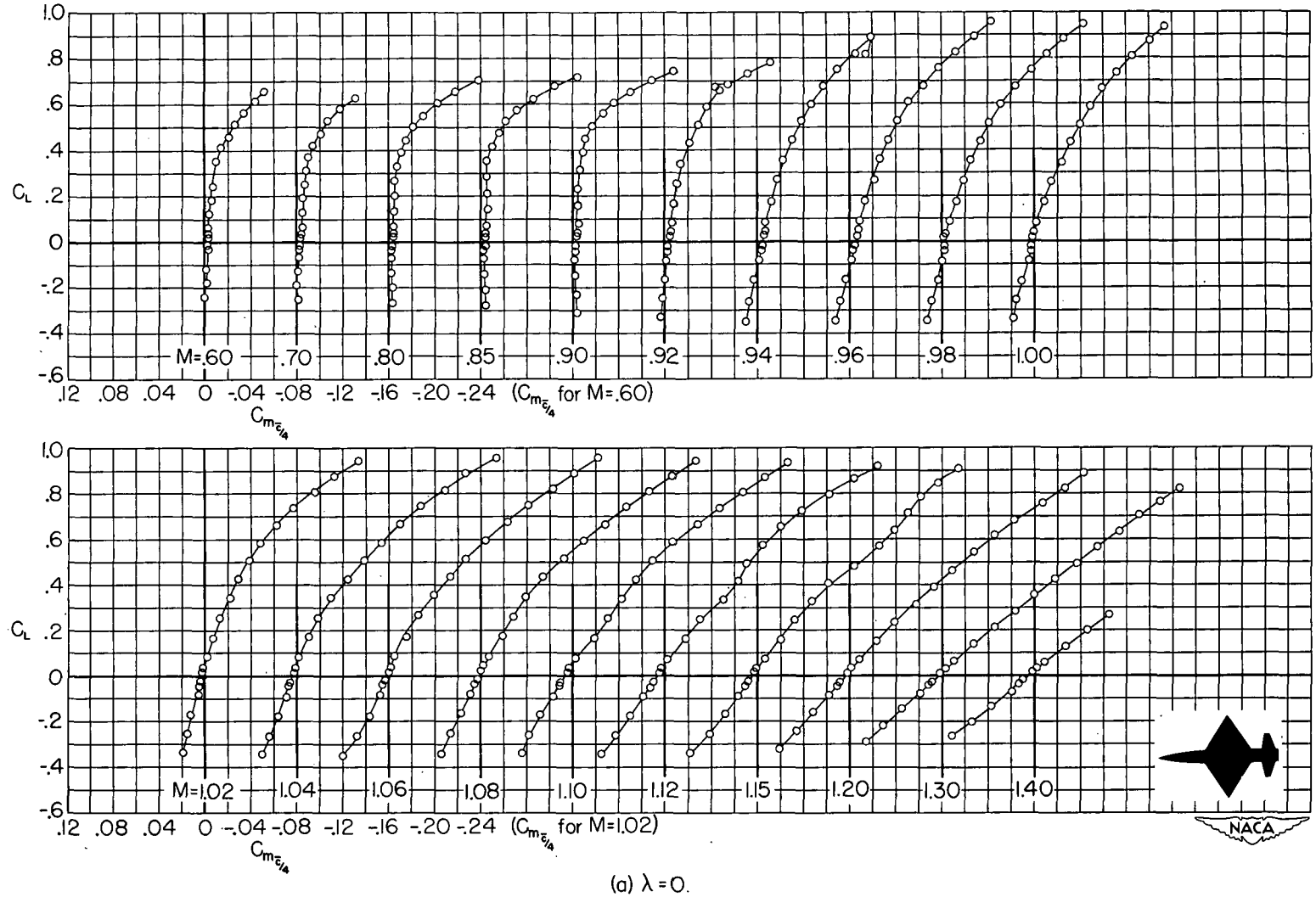

(a) $\lambda = 0$.

Figure 9.- Variation of lift coefficient with pitching-moment coefficient at constant Mach number for an unswept wing-body-tail combination.

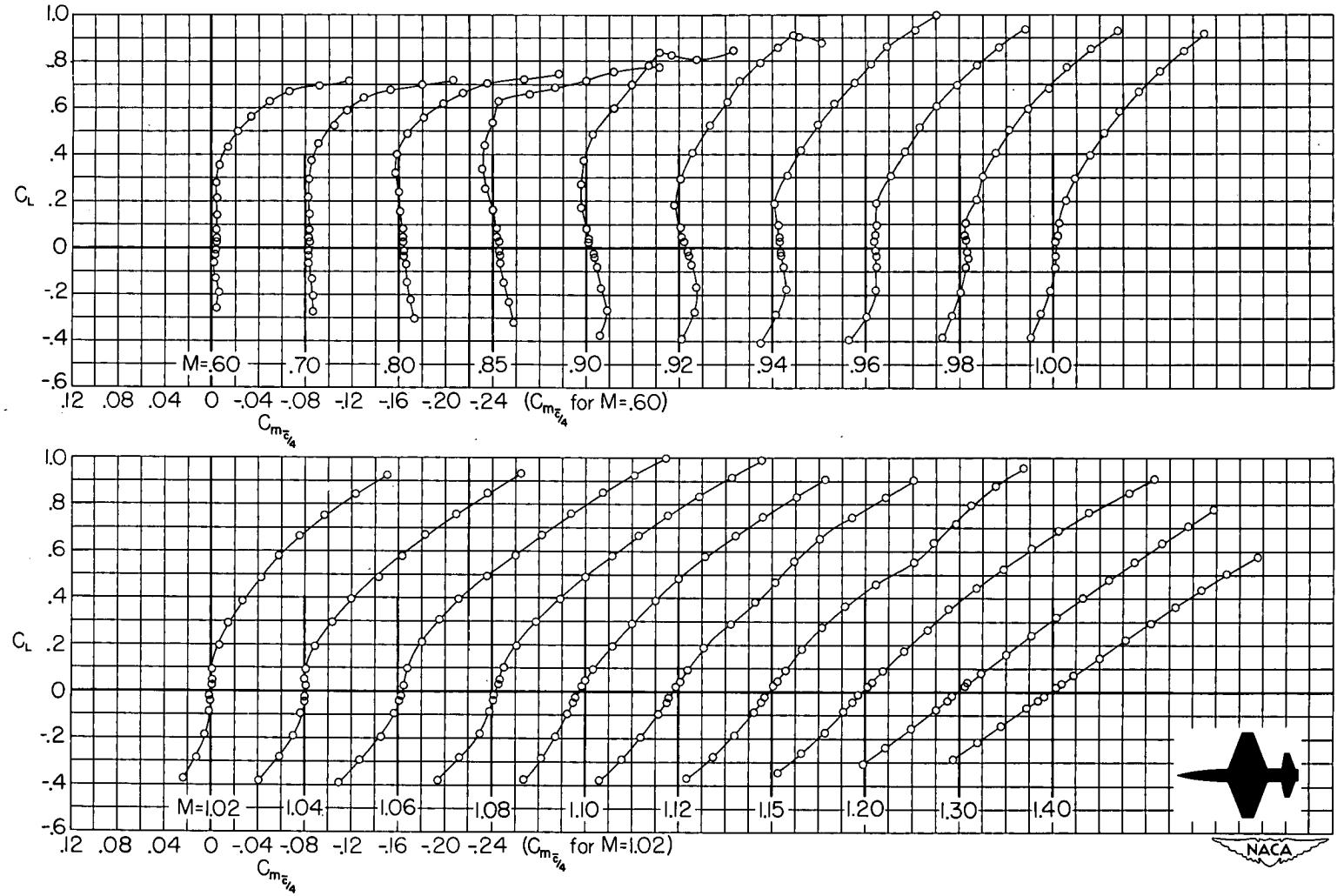

(b) $\lambda = 0.25$.

Figure 9.- Continued.

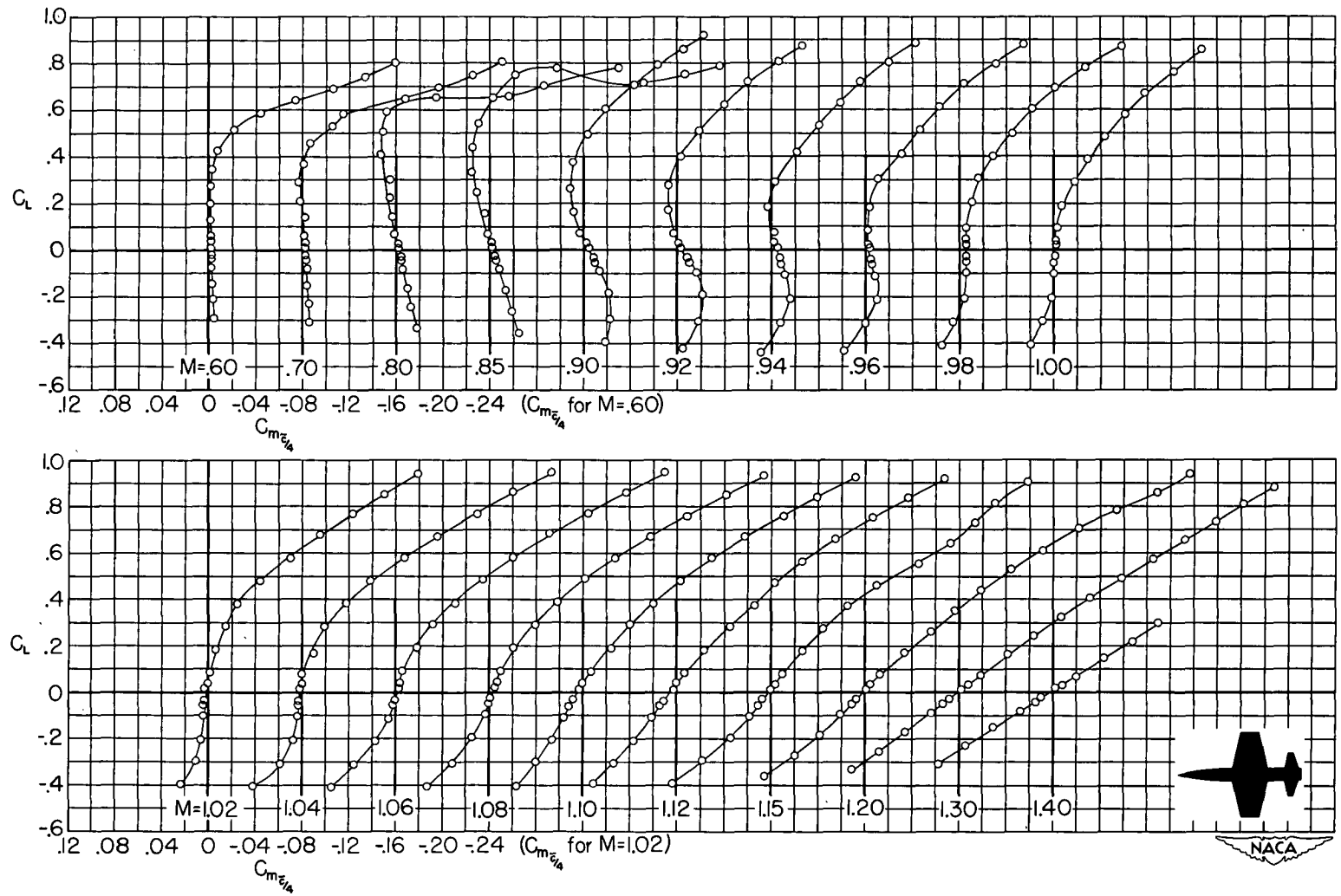

(c) $\lambda = 0.50$.

Figure 9.- Continued.

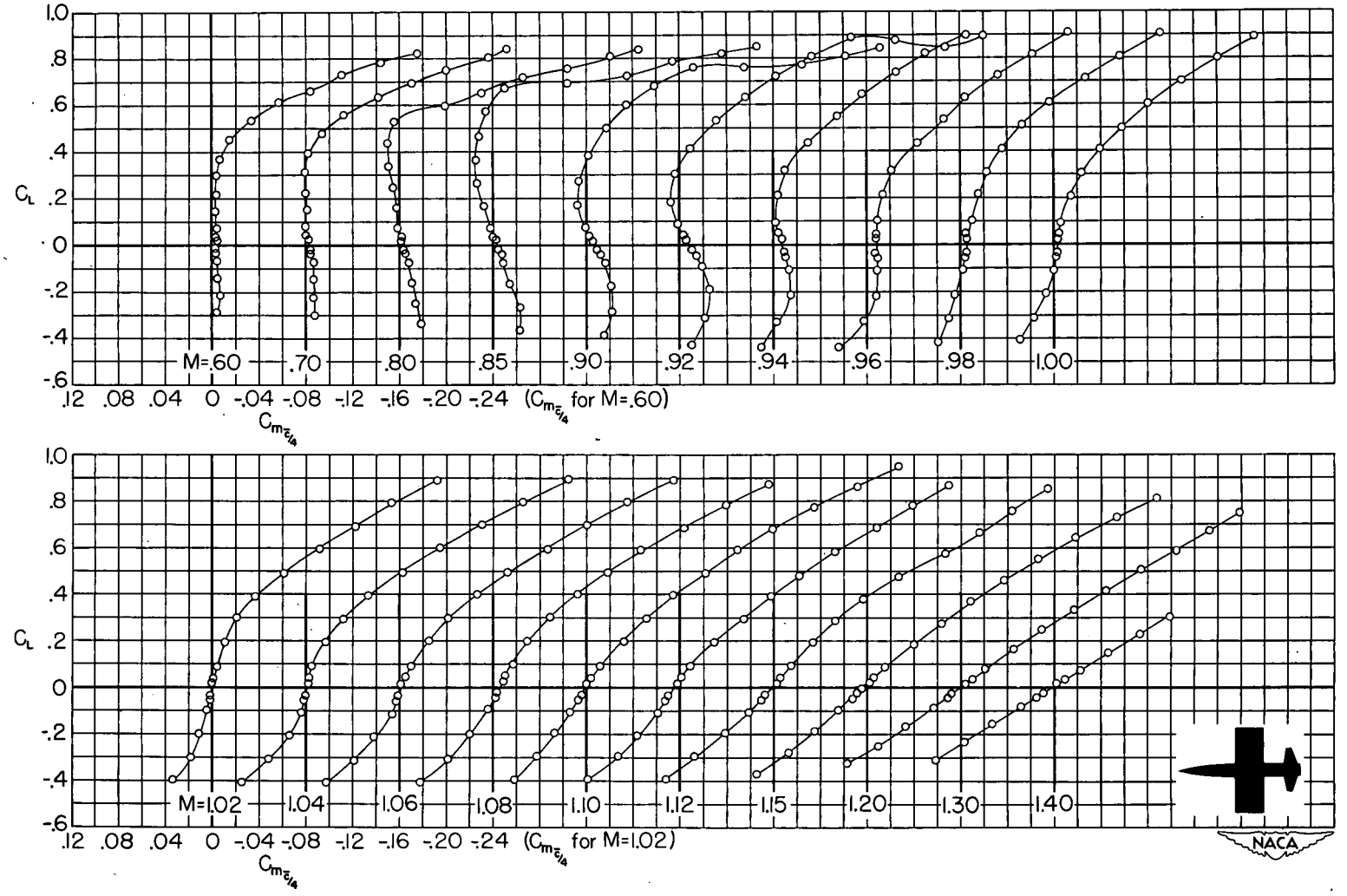

(d) $\lambda = 1.00$.

Figure 9.- Concluded.

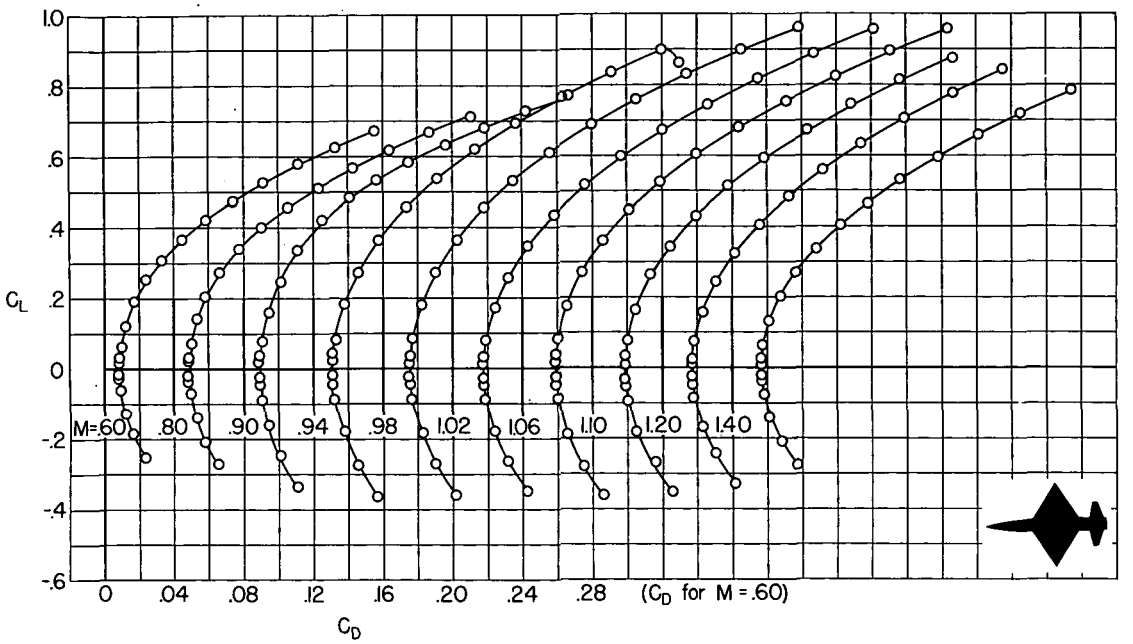

(a) $\lambda = 0.$

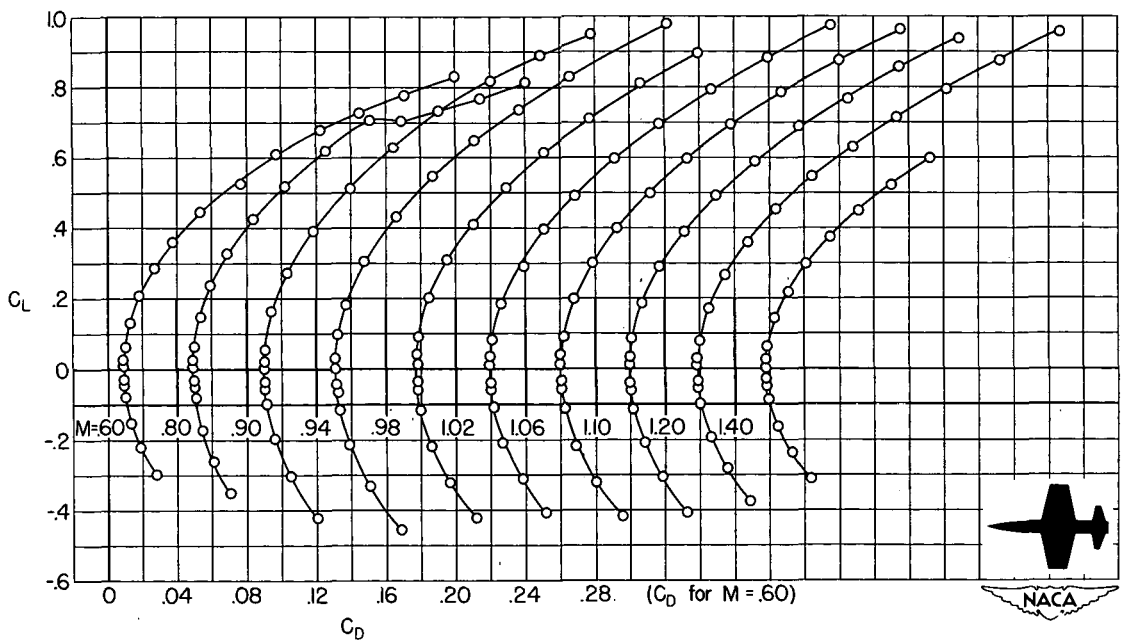

(b) $\lambda = 0.50.$

Figure 10.- Variation of lift coefficient with drag coefficient at constant Mach number for an unswept wing-body-tail combination.

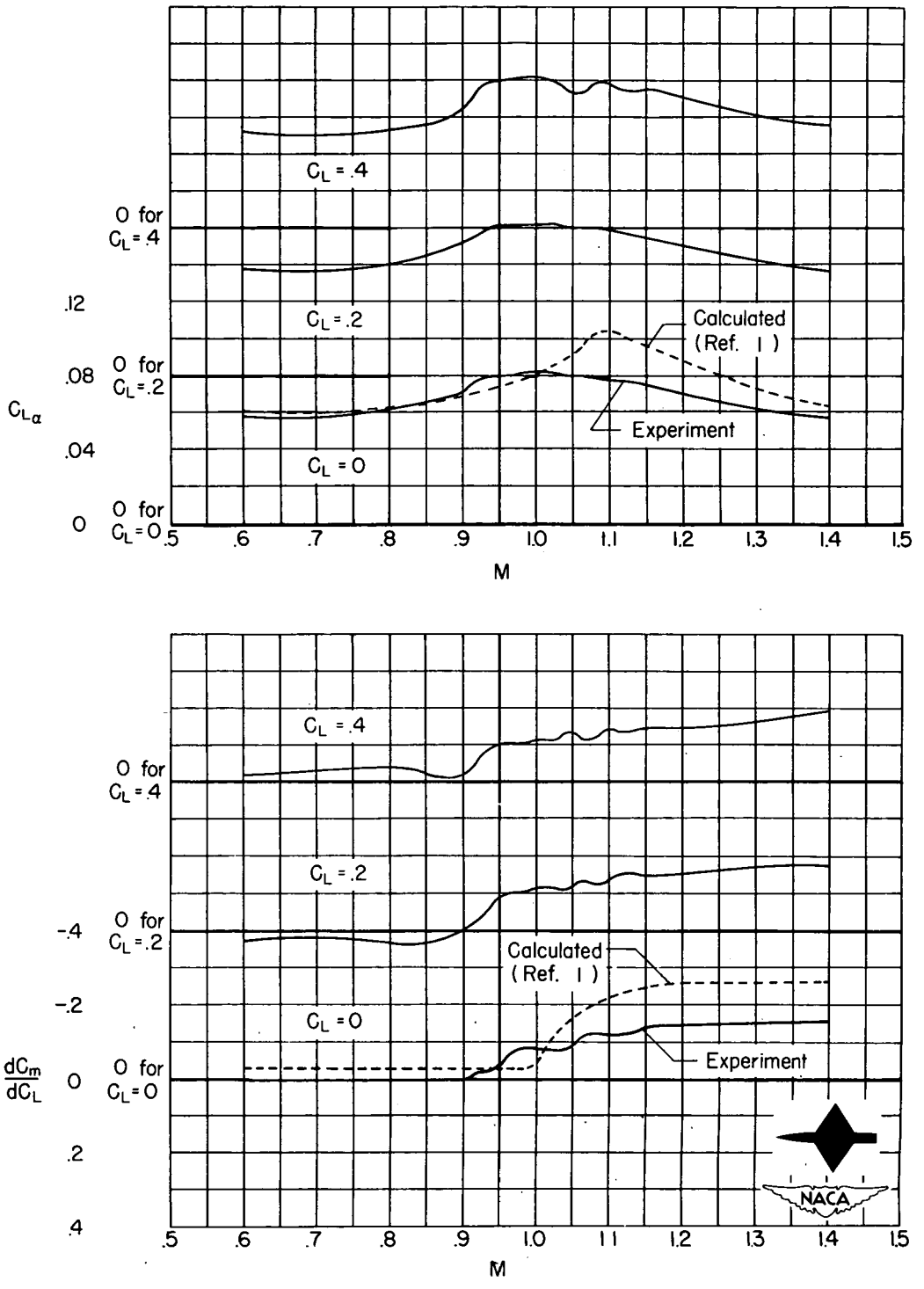

(a) $\lambda = 0$.

Figure 11.- Variation of lift-curve slope and pitching-moment-curve slope with Mach number for an unswept wing-body combination.

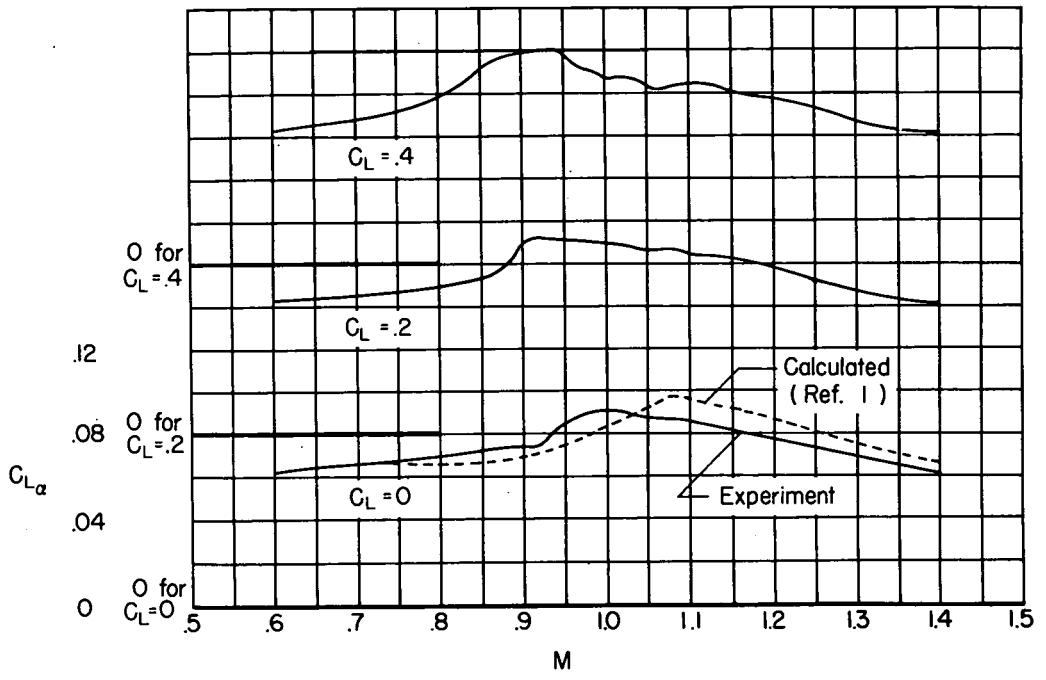

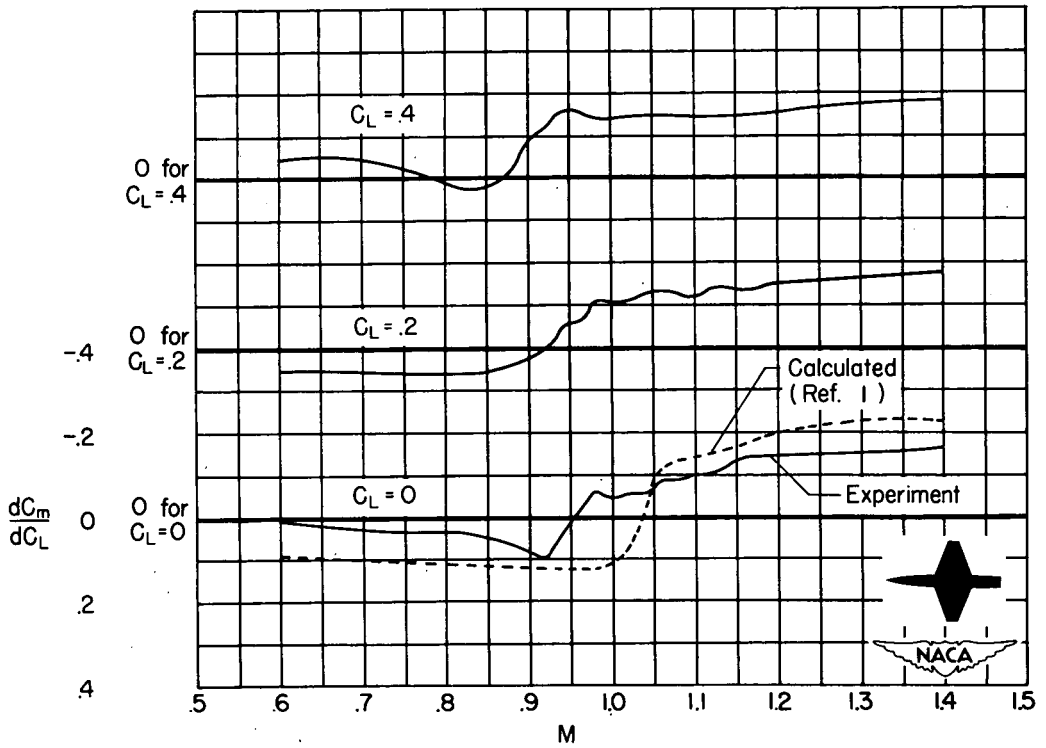

(b) $\lambda = 0.25$.

Figure 11.- Continued.

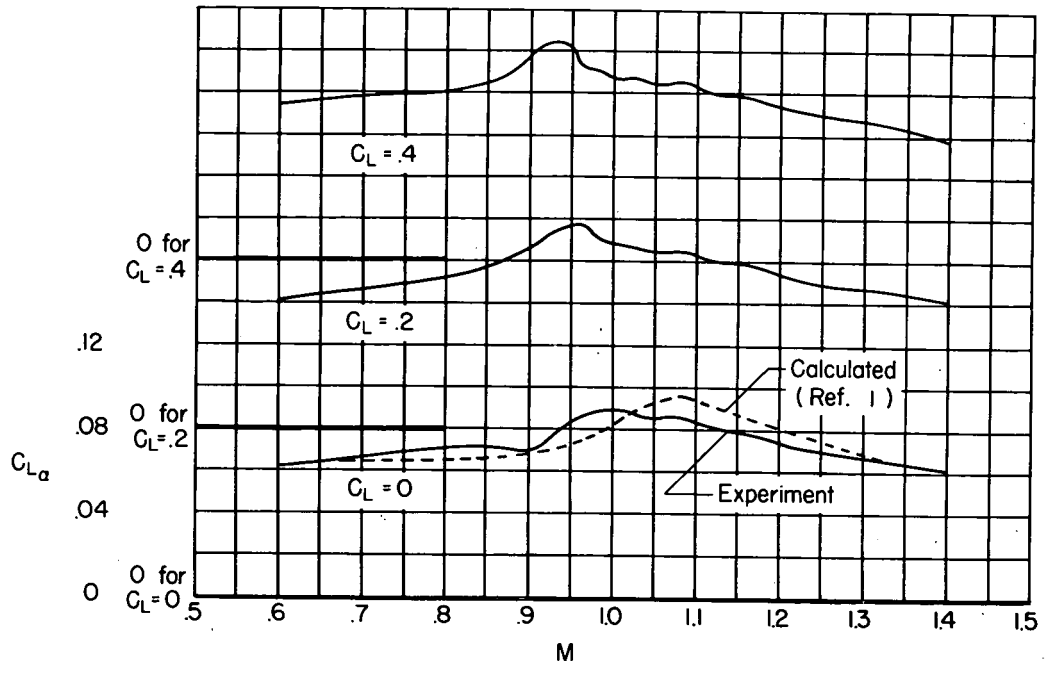

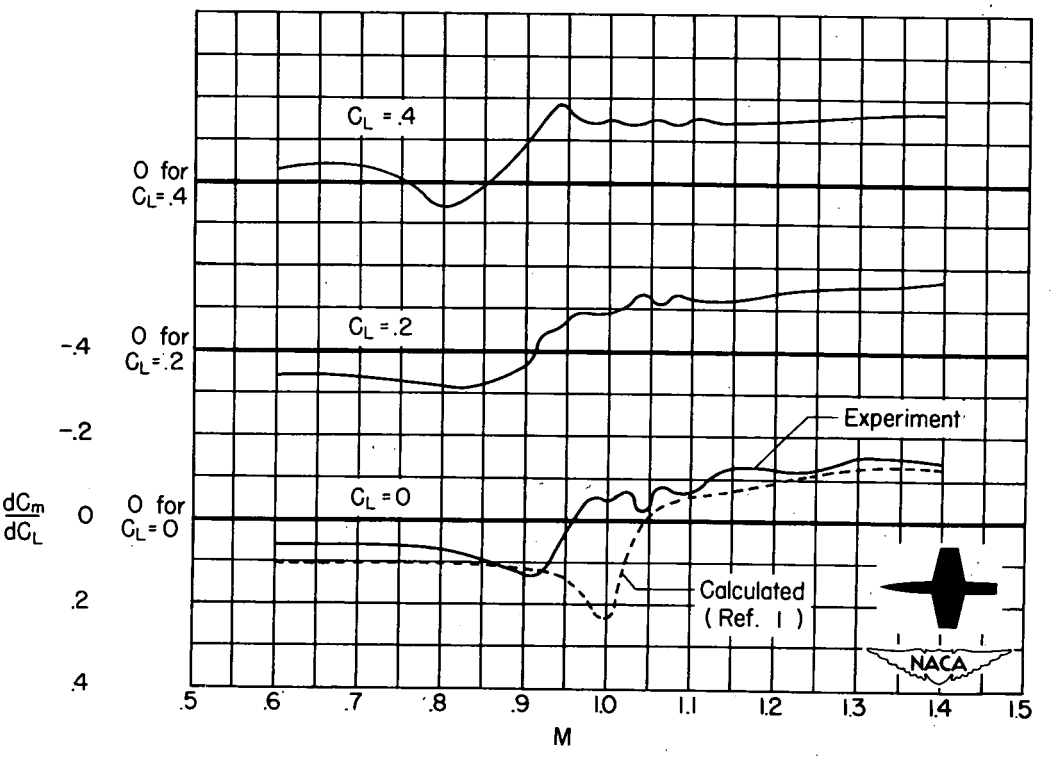

(c) λ = 0.50.

Figure 11.- Continued.

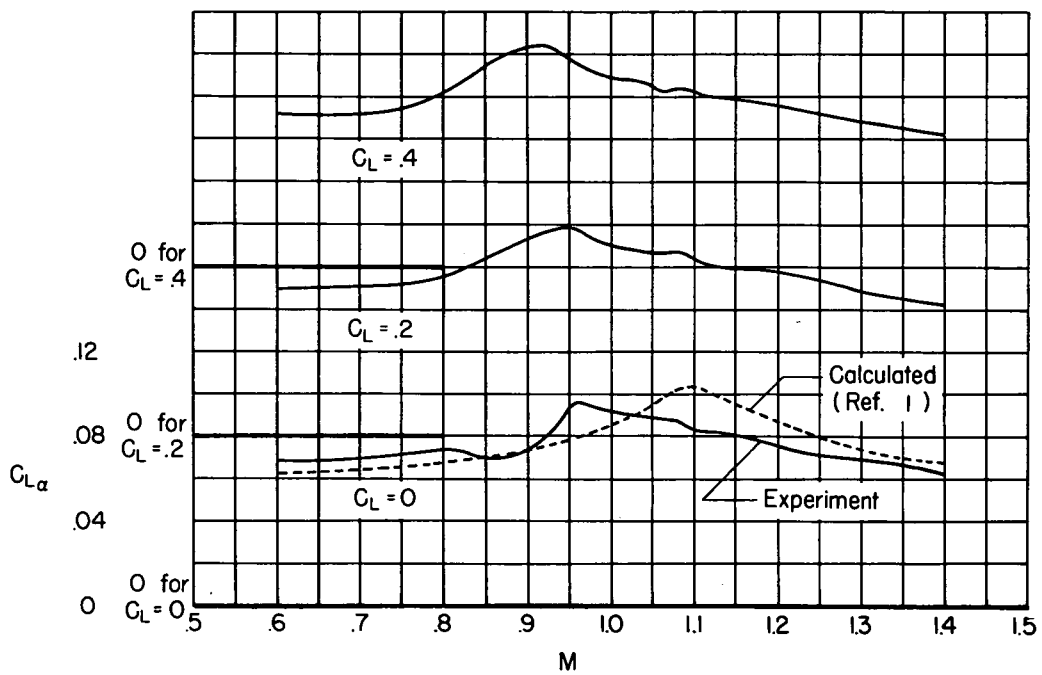

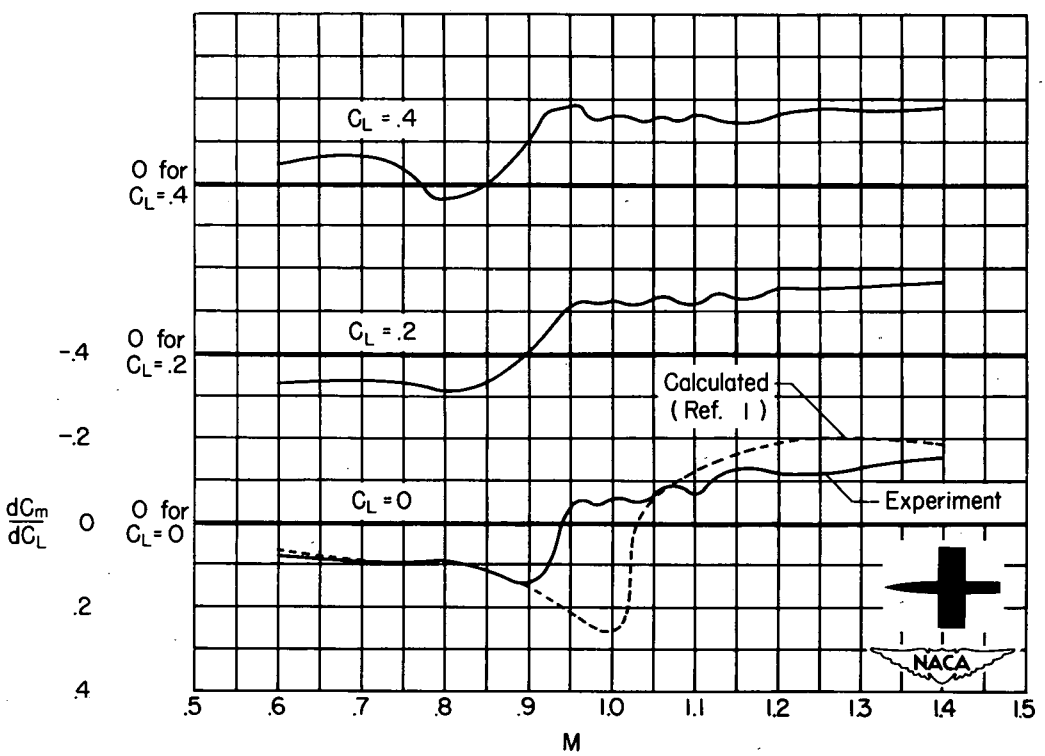

(d) λ = 1.00.

Figure 11.- Concluded.

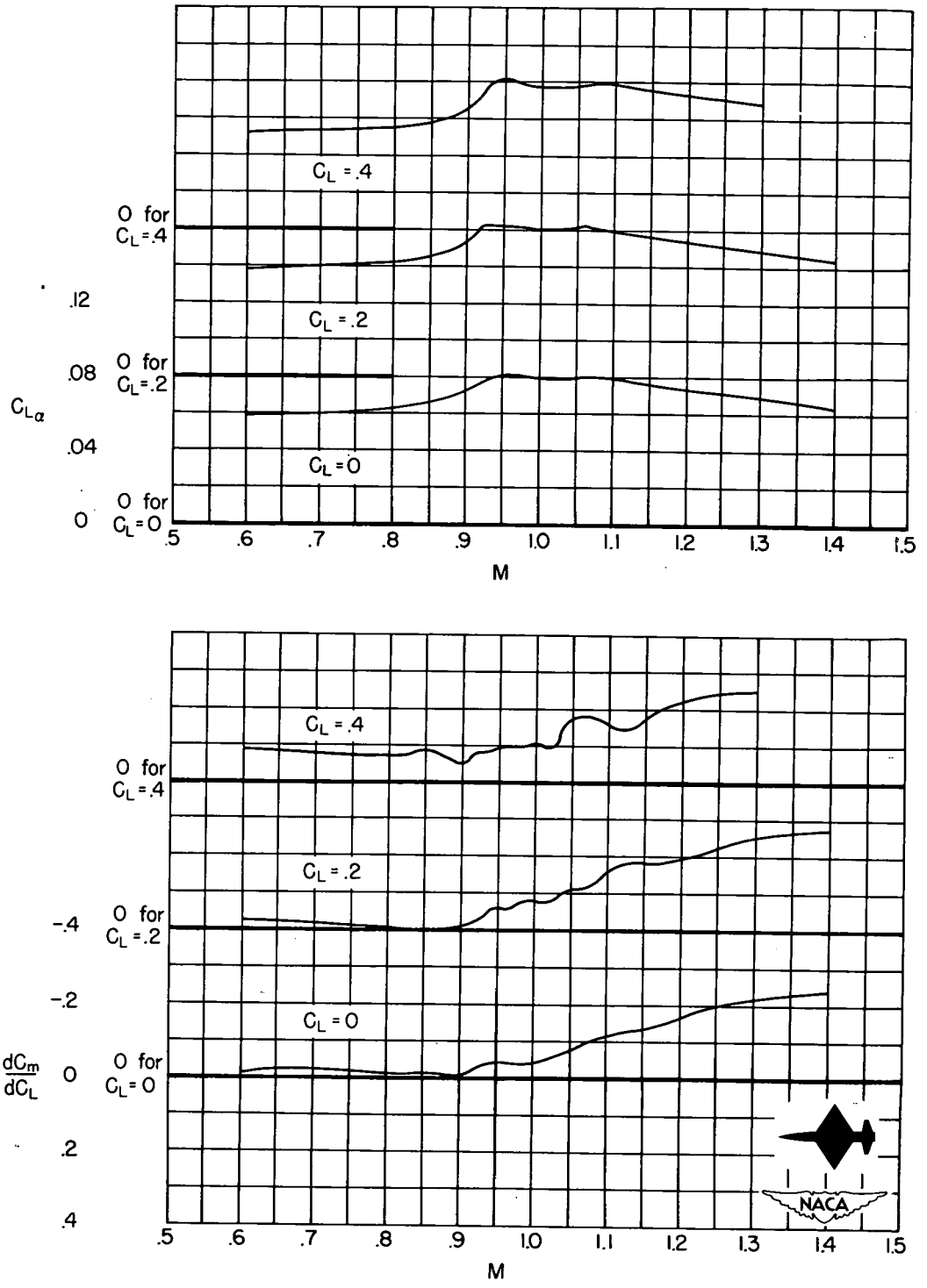

(a) $\lambda = 0$.

Figure 12.- Variation of lift-curve slope and pitching-moment-curve slope with Mach number for an unswept wing-body-tail combination.

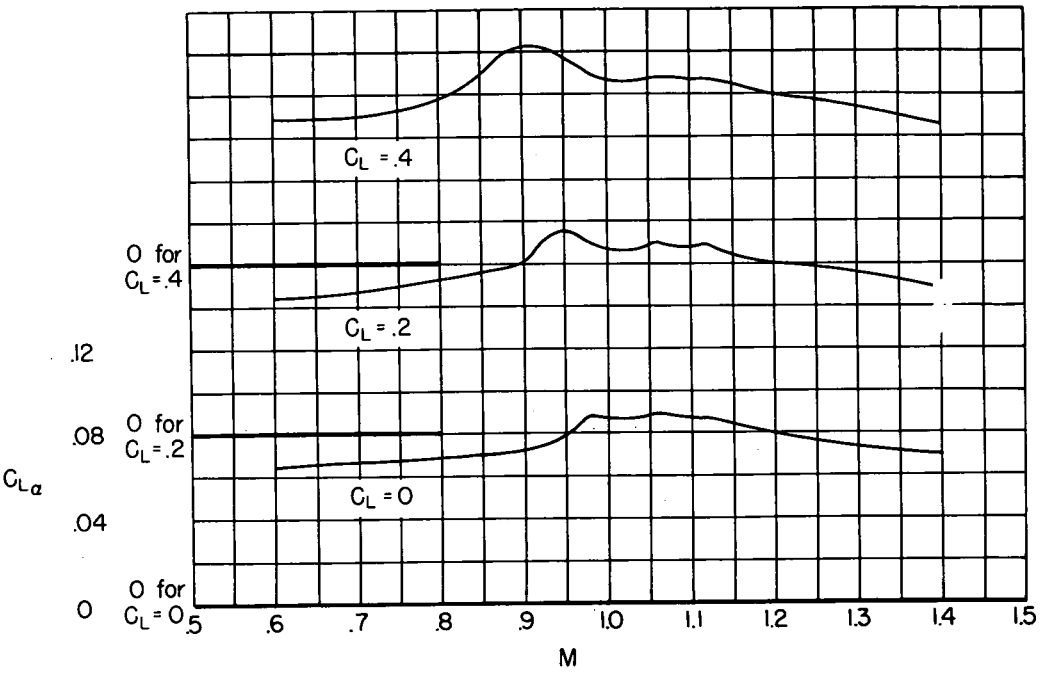

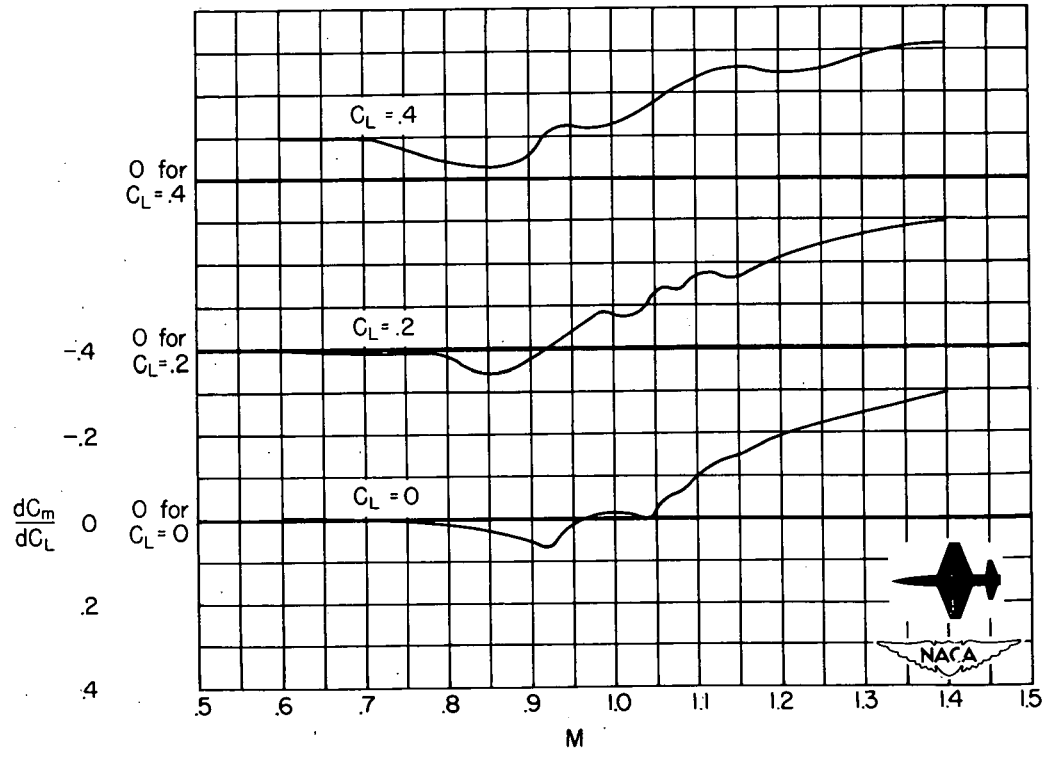

(b) $\lambda = 0.25$.

Figure 12.- Continued.

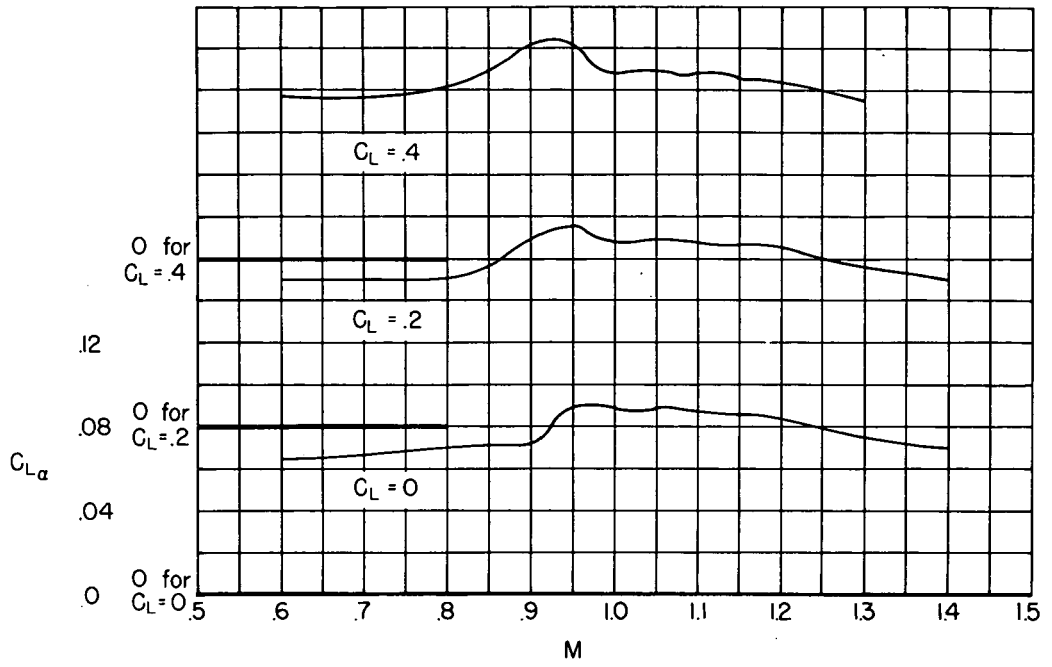

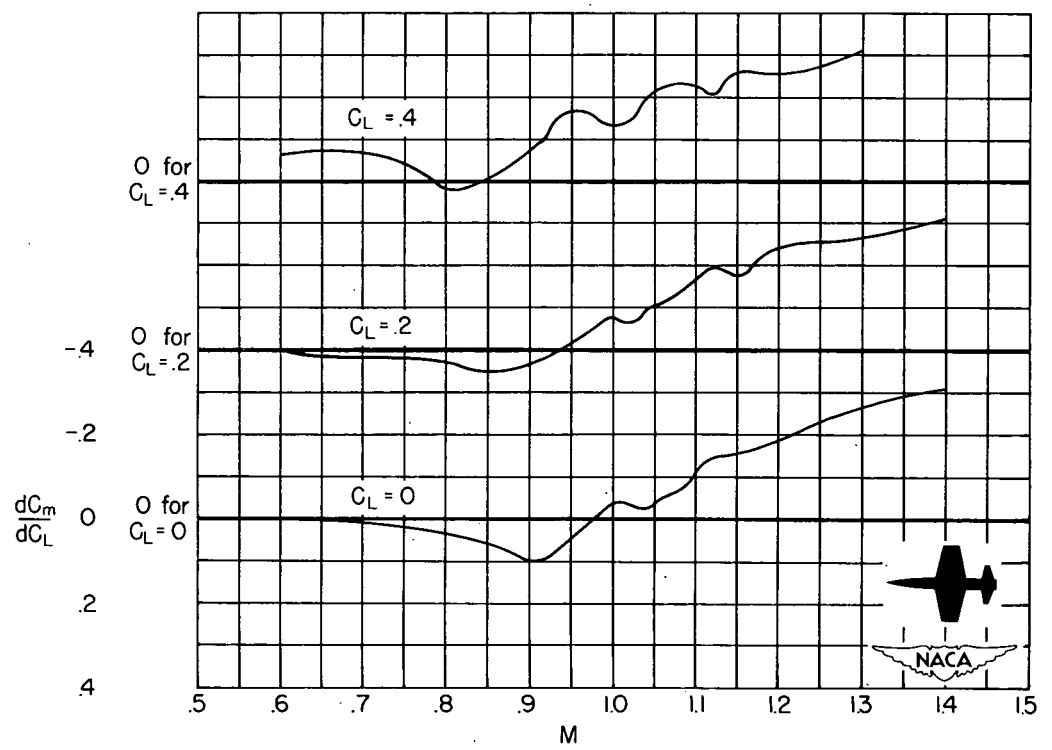

(c) λ = 0.50.

Figure 12. - Continued.

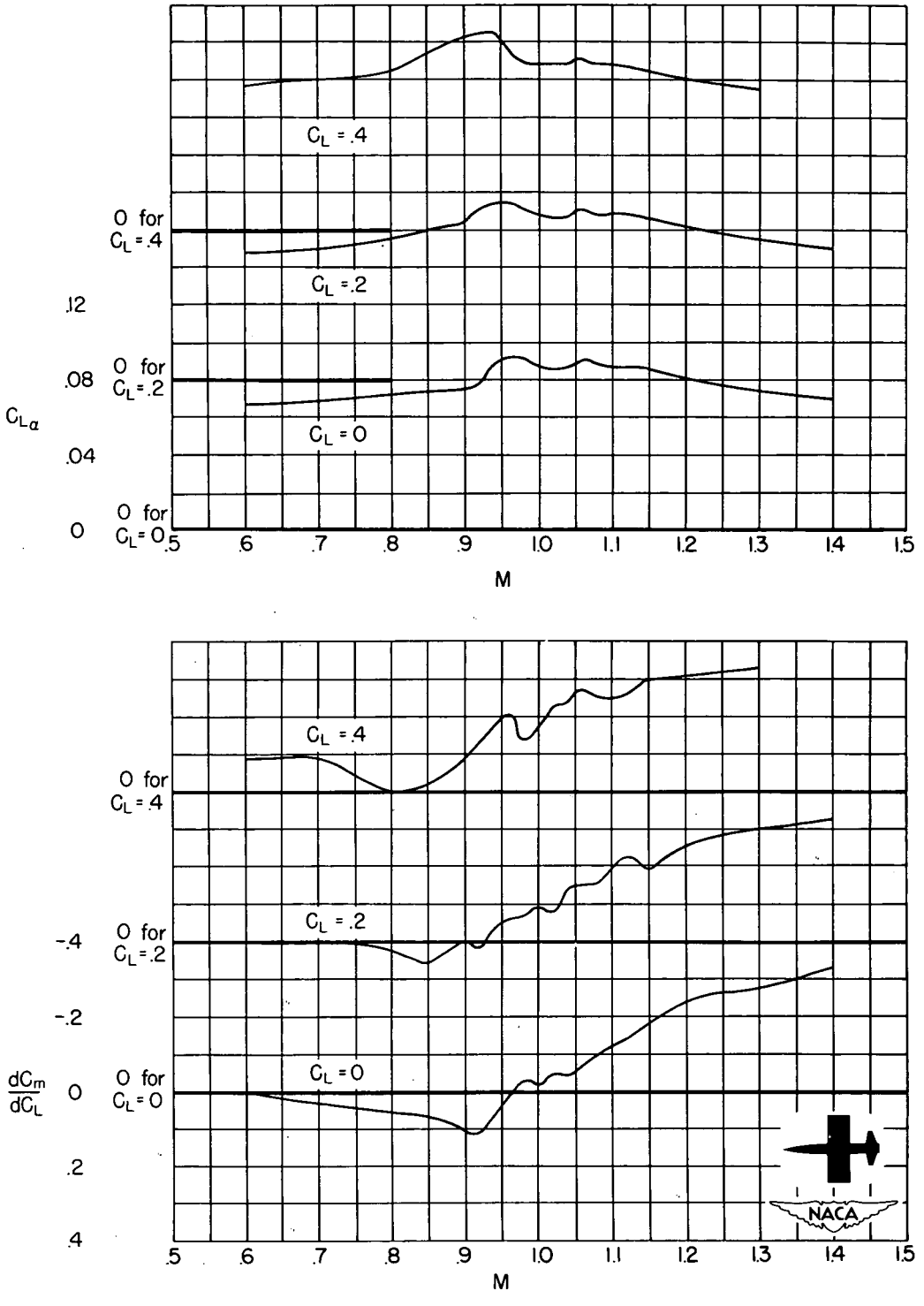

(d) λ = 1.00.

Figure 12.- Concluded.

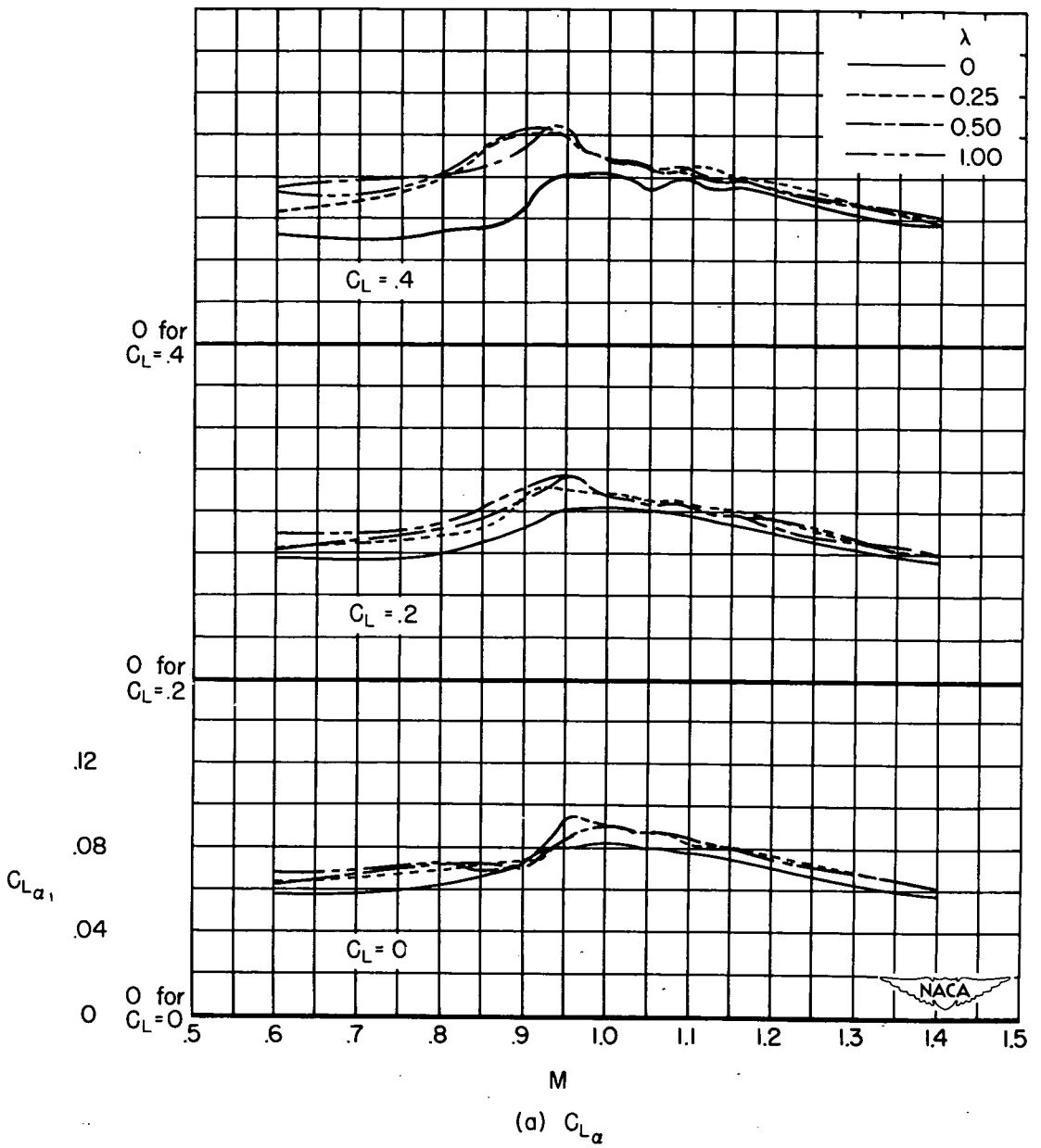

(a) C_{L_α}

Figure 13.- Effect of taper ratio on the variation of C_{L_α} and $\Delta\left(\frac{dC_m}{dC_L}\right)_M$ with Mach number at three lift coefficients for an unswept wing-body combination.

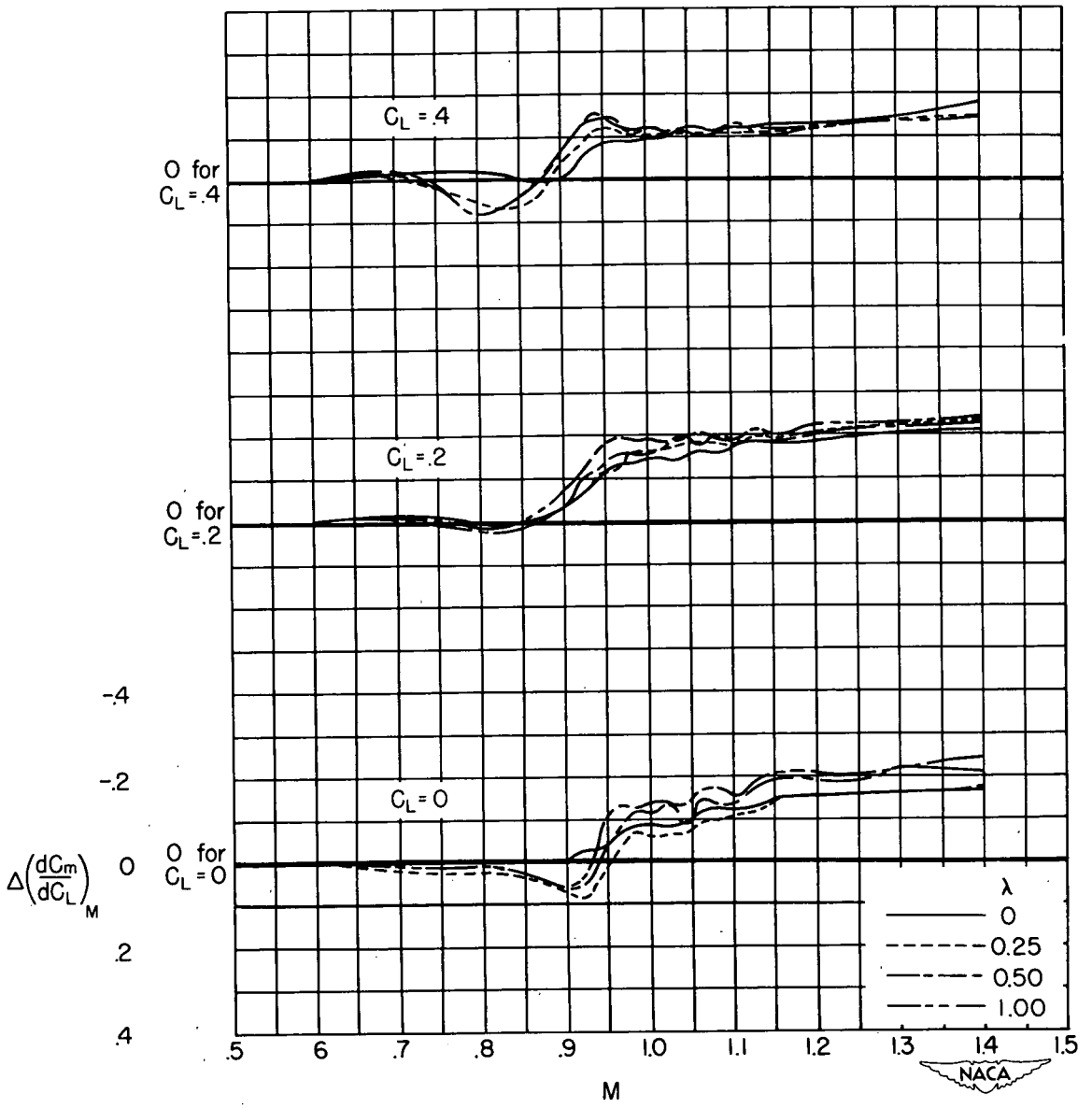

(b) $\Delta\left(\frac{dC_m}{dC_L}\right)_M$

Figure 13.- Concluded.

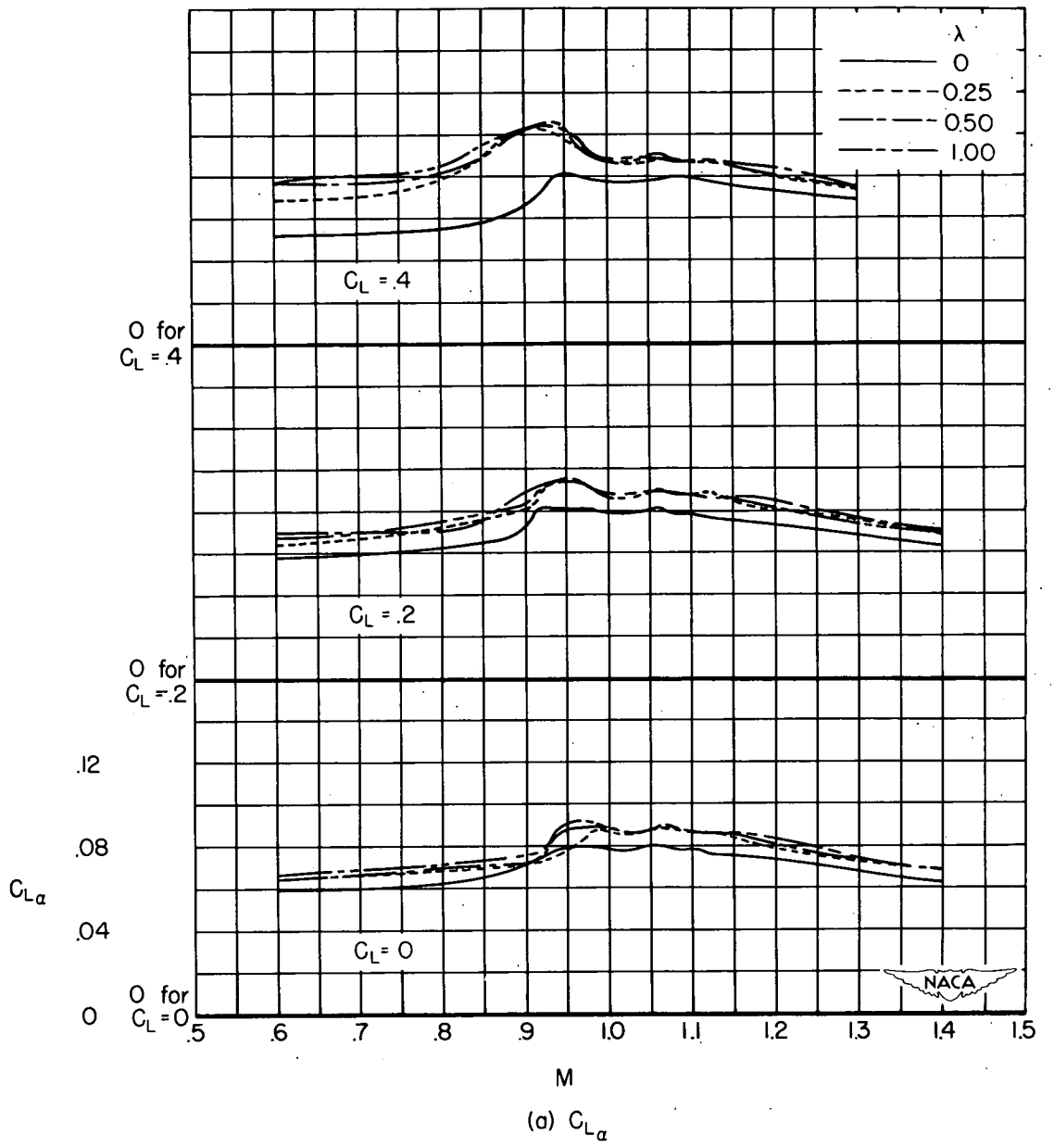

(a) C_{L_α}

Figure 14.- Effect of taper ratio on the variation of C_{L_α} and $\Delta\left(\frac{dC_m}{dC_L}\right)_M$ with Mach number at three lift coefficients for an unswept wing-body-tail combination.

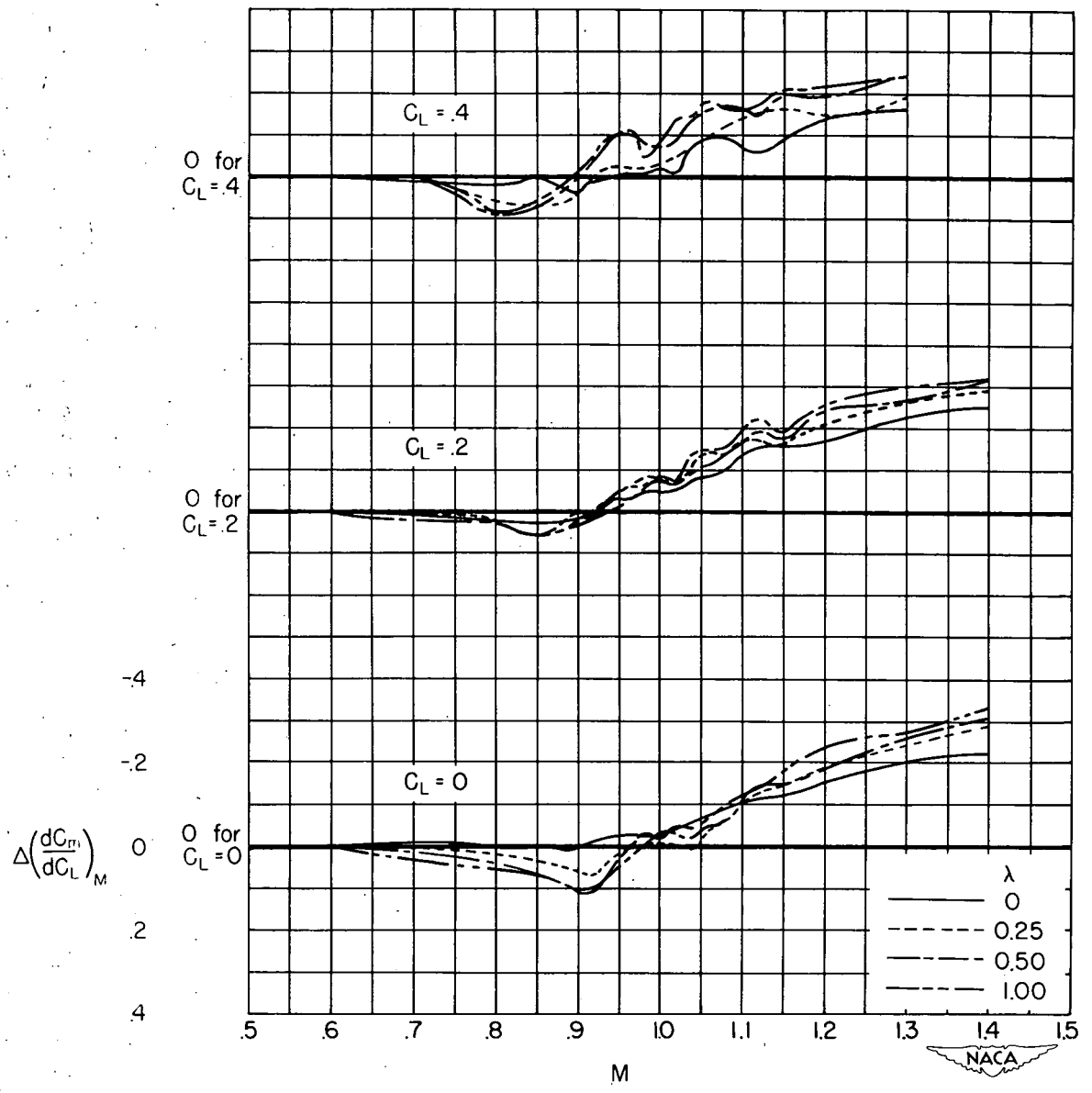

(b) $\Delta\left(\frac{dC_m}{dC_L}\right)_M$

Figure 14.- Concluded.

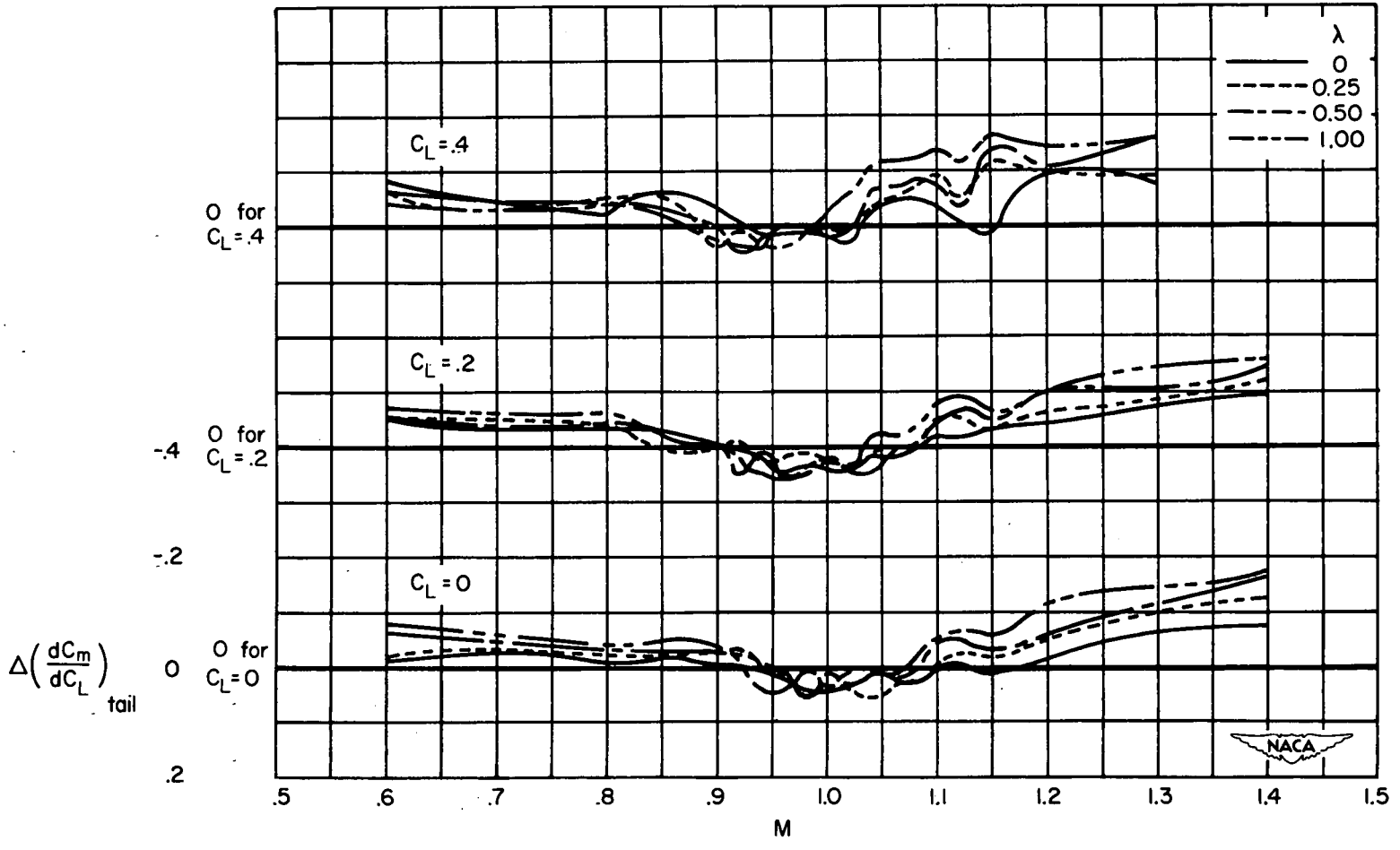

Figure 15.- Effect of taper ratio on the variation of $\Delta\left(\frac{dC_m}{dC_L}\right)_{tail}$ with Mach number at three lift coefficients for an unswept wing-body-tail combination.

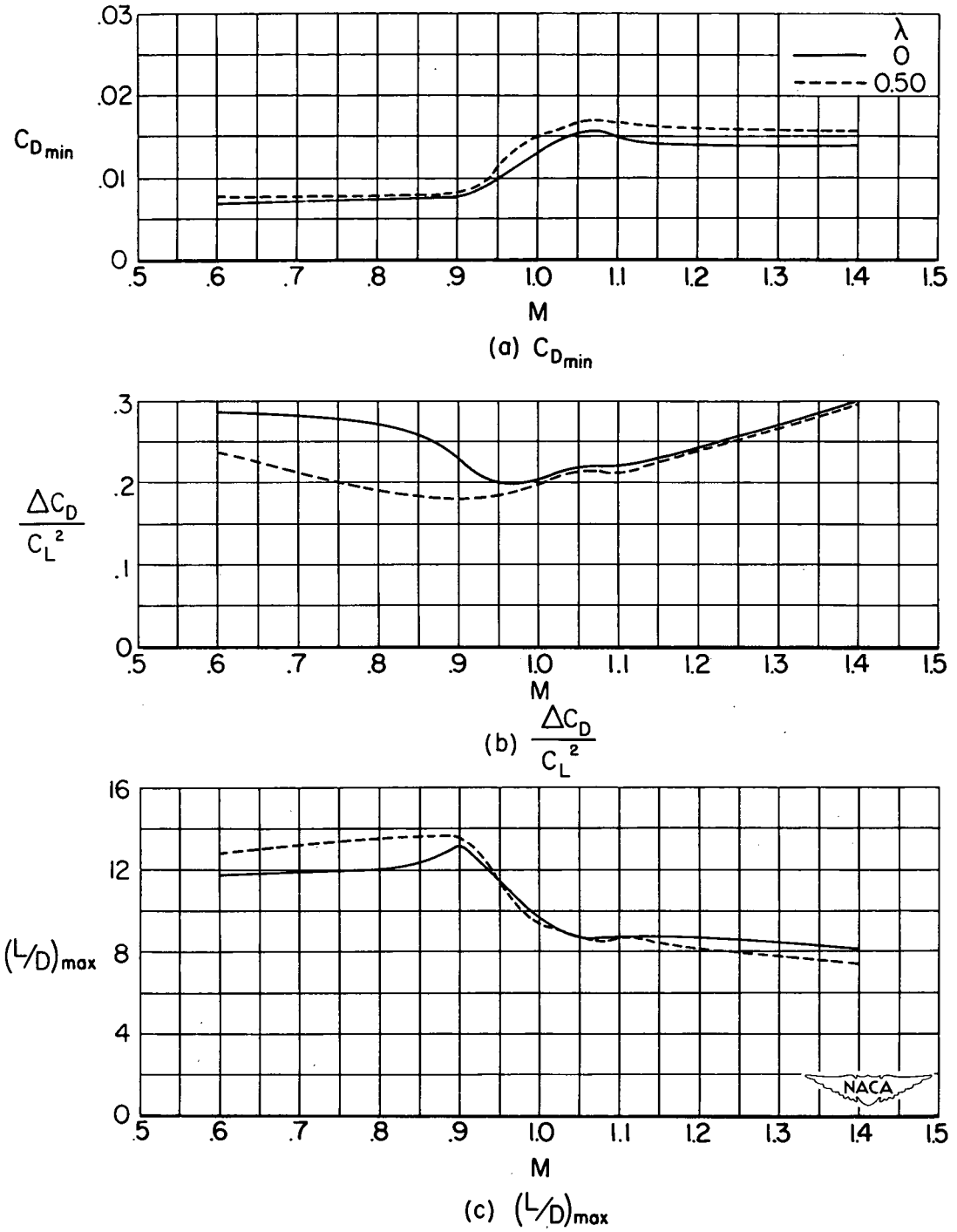

Figure 16.- The effect of taper ratio on the variation of minimum drag coefficient, drag-rise factor and maximum lift-drag ratio with Mach number for an unswept wing-body combination.

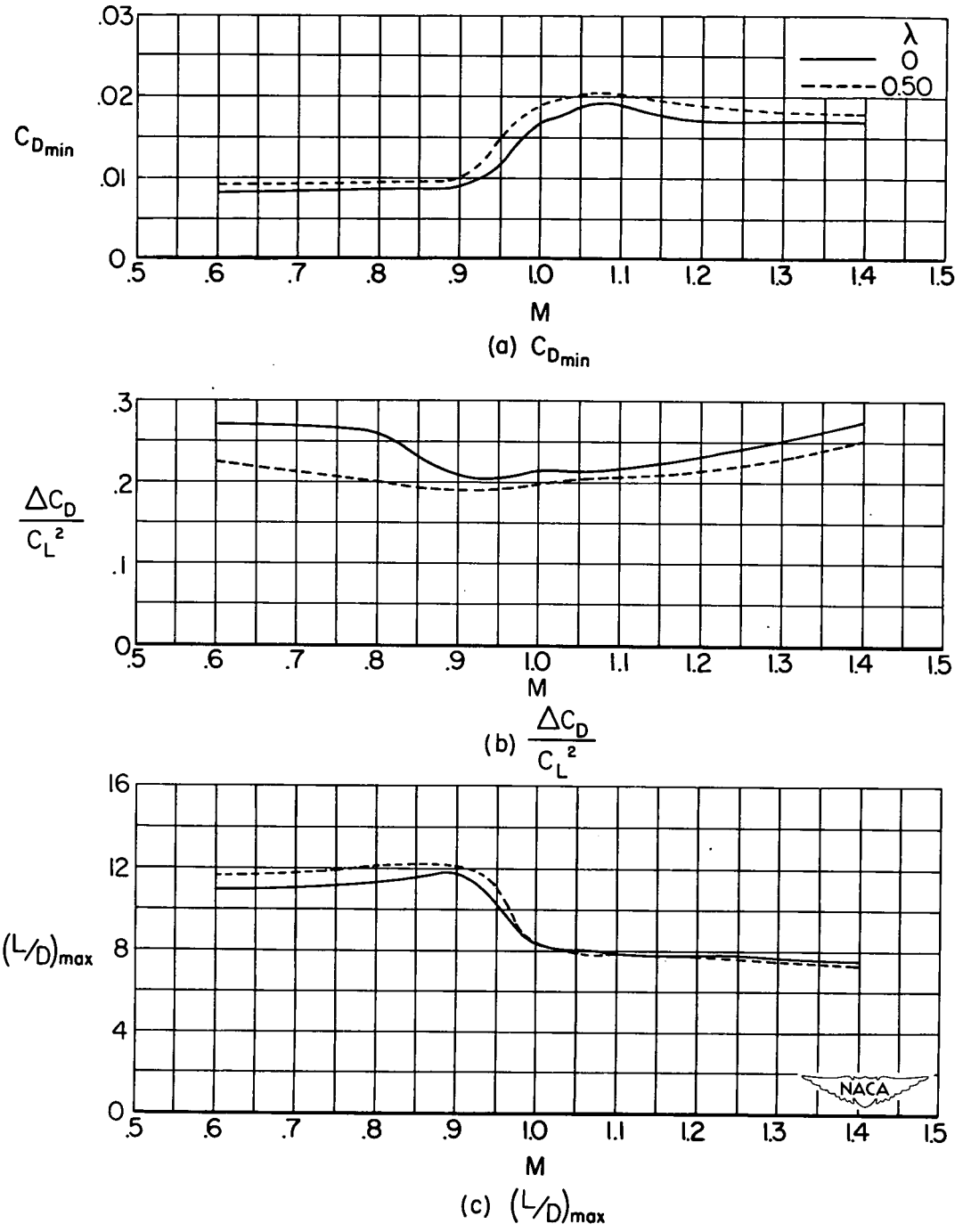

Figure 17. - The effect of taper ratio on the variation of minimum drag coefficient, drag-rise factor and maximum lift-drag ratio with Mach number for an unswept wing-body-tail combination.